Elsevier Editorial System(tm) for Engineering Structures
Manuscript Draft

Manuscript Number: ENGSTRUCT-D-16-00912R1

Title: Structural elements made with highly flowable UHPFRC: correlating Computational Fluid Dynamics (CFD) predictions and non-destructive survey of fiber dispersion with failure modes

Article Type: Research Paper

Keywords: UHPFRC; flow induced fiber orientation; computation fluid dynamics; non destructive fiber monitoring; slabs; structural design

Corresponding Author: Professor. Liberato Ferrara, PhD

Corresponding Author's Institution: Politecnico di Milano

First Author: Liberato Ferrara, PhD

Order of Authors: Liberato Ferrara, PhD; Massimiliano Cremonesi, assistant professor; Marco Faifer, assistant professor; Sergio Toscani, assistant professor; Luca Sorelli, professeur agrege; Marc-Antoine Baril, PhD; Julien Réthoré, Research Associate - CNRS; Florent Baby, Ingénieur de recherche en Ouvrages d□Art; François Toutlemende, Délégué scientifique et international; Sebastien Bernardi, Technical Head

Abstract: Structural design with highly flowable Fibre Reinforced Concrete has to duly take into account the preferential alignment of fibers, which can be governed through the rheological properties of the fluid mixture and the casting process and by the geometry of the structure. The possibility of predicting the fiber alignment, by tailoring the casting process, and of non-destructively monitoring it, can foster more efficient structural applications and design approaches. Focusing on UHPFRC slabs with pre-arranged casting defects, the flow-induced alignment of the fibers has been predicted by means of a suitable CFD modelling approach and hence monitored via a non-destructive method based on magnetic inductance properties of the fiber reinforced composite. The comparison between the assessed data on the fibre orientation and the crack patterns as visualized by image analysis supports the effectiveness of casting flow modelling and non-destructive fiber dispersion monitoring in supporting the structural design of elements made with highly flowable fiber reinforced cementitious composites.

Response to the reviewers of the manuscript ENGSTRUCT D-16-00912

Structural elements made with highly flowable UHPFRC: can Computational Fluid Dynamics (CFD) and non-destructive survey of fiber dispersion complement structural design in predicting failure modes?

authored by: *Liberato Ferrara[1], Massimiliano Cremonesi[1], Marco Faifer[2], Sergio Toscani[2], Luca Sorelli[3], Marc-Antoine Baril[3], Julien Réthoré[4], Florent Baby[5], François Toutlemonde[5] and Sébastien Bernardi[6].*

submitted for publication to Engineering Structures

The authors thank the reviewers for the time they have dedicated to read their manuscript and for the insightful comments they have made and for the overall evaluation of the manuscript.

The authors have taken in high consideration all the comments, mainly made by the second reviewers, and have addressed them in the revised version of the manuscript, which is now resubmitted.

In detail:

RESPONSE TO REVIEWER 1

- The authors agree that citing "structural design" in the title may rise some expectations in the reader which the paper does not fully address. In view of this the tile has been modified as follows
  Structural elements made with highly flowable UHPFRC: correlating Computational Fluid Dynamics (CFD) predictions and non-destructive survey of fiber dispersion with failure modes?
  (see also response to 1st general remark of reviewer 2)
- The thickness of the slab (30 mm) has been declared
- Reference [93] (which has now become reference [94]) contains details about the test set-up and the mechanical test results with elaboration of the digital image correlation measurements of the cracks, which in this paper are taken as reference and simply compared with CFD predictions and ND fiber dispersion monitoring.
- The citation by Svec has been added. As for the other reference cited by the reviewer, the authors are doubtful whether to cite or not since it is likely an internal publication which is not indexed nor widely available.
- With reference to the slab with the defect at 1/3 of the side it is not true that the defect does not affect the crack pattern; even in the major crack does not develop along the casting defect line, the presence of the same defect prevents the radial crack pattern to fully develop as in the reference slab. This aspect has been clarified in the text.

RESPONSE TO REVIEWER 2

General comments:

1. Addressed; see also response to reviewer 1

2. The issue has been addressed by adding the following sentences in section 5:
This approach, though simplified, is able to provide the information about the trend of spatial orientation of fibers in the structural element as cast which may be sufficient for structural applications such as the ones herein dealt with. It is worth remarking that the benefits of fibers are best exploited in a structural configuration allowing for sufficient redistribution of post-cracking stresses, as the slabs here tested. In these cases "local" or "pointwise" information about fiber concentration and orientation may be redundantly detailed, since right the aforementioned stress redistribution capacity would allow to shadow concentrated defects, still remaining sensitive to a major "average spatial" trend in spatial dispersion and orientation of the fibers.

3. Being this a case study the authors have employed the knowledge developed in previous years of research and work; the fundamental information needed to understand the content of this paper has been clearly reported, in the authors' opinion; the reader is referred to the literature for knowledge about model and approach formulation which would have unnecessarily burdened the readability of the paper.

4. The study the authors speaks about is on going, dealing with multiple testing/prediction/analysis techniques, which has led the authors to publish the results into different parts.

5. Done; thanks to the reviewer for having anyway done the work also in absence of page and line numbers (some journals provide this in building up the pdf file for review).

Specific comments:

1. The comment has been addressed by adding the following sentences as required by the reviewer:
Preferential orientation of fibers also jeopardize the isotropic material behavior assumption; the resulting even strongly orthotropic mechanical behavior of the material has to be duly taken into account in structural design, most of all when dealing with slab and shell structures which experience complex biaxial stress field arising from different load combinations.

2. It has been speficied that Xrays mainly work in the case of steel fibers

3. It has been specified that it is the "X-ray" absorption capacity

4. As a matter of fact there are several cases of highly effective HPFRCC salso with one type of fibers. The authors are not aware of any application of any method for ND fiber survey with hybrid reinforcement of fibers. Anyway the following clarification has been added:
", which may affect the possibility to apply the method to the case of hybrid fiber reinforcement".

5. Since the method has been shown to be sensitive to both concentration and orientation the sentence has been modified as follows:
"The method has been extensively employed to assess the influence of the fresh state performance on the dispersion and orientation of the fibers [12], clearly highlighting the better uniformity in fiber dispersion achievable through FR-SCC, together with a sensitivity to flow induced fiber alignment."

6. The sentence has been modified as follows:
"Since the (known) fiber aspect ratio governs the capacitive behavior of the fibers and of the fiber reinforced composite, The the local average concentration of fibers could be assessed by assuming a random fiber orientation. In view of this and because of the known fiber geometry (aspect ratio) which governs their capacitive behavior, but the method is not sensitive to a preferential alignment of the fibers.".

7. It is actually the velocity vector; modified accordingly

8. Modified as follows:
   "The methodology consists on three steps: firstly, the casting process has been modeled by means of a Computational fluid Dynamics (CFD) modeling tool, employing a Lagrangian approach based on Particle Finite Element method [89, 90], and flow-induced orientation of fibers has been "guessed" through the velocity vector patterns of the simulated casting process."

   This is just preliminary description; details follow

9. It is French Association of Civil Engineering (acronym in French); simply modified into "French recommendations"
10. This is quite an "instrumental" question. Any person well versed in finite element analysis is aware of the concept that the "element" size is a function of the cubic root of the element volume in the case of "non-cubic" elements in 3D and in 2D, when non square elements are used, is a function of the square root of the element area.
11. Removed
12. The comments is truly non persuasive. After the sentence the reviewer cite the authors summarize the procedure for measuring and reducing data (the references are cited for completeness). It seems truly strange that the reviewer says that the procedure is not summarized. Anyway, the sentence, for the sake of clarity, has been modified as follows:
    "Non-destructive monitoring of fiber dispersion and orientation was performed on the slabs, once hardened, according to the methodology proposed in [71, 72], and hereafter briefly summarized."
13. 1st question: yes (reference cited); 2nd question: the response is the the following sentence "nonetheless …".
14. In this case the in plane orientation is the only necessary information because of the small slab thickness, which is a typical thickness for UHPFRCC applications. Other cases are out of the scope of the paper.
15. The authors have added the following sentence to explain the choiceof the measuring grid and comment, as required, Figure 6 (now Figure 5)
    "The choice of the measuring grids was dictated by the geometry of the slab and by the position of the casting defect, as well as by the need of garnering information on fiber dispersion and orientation also across the same casting defects as above."
    The choice of the grids is anyway self evident.
16. Added in modified Figure 6a (now Figure 5a).
17. This was done in the calibrations study (refs 71 and 72); the calibration procedure is briefly summarized in this paper.
18. The authors do not agree; the snapshots of the casting flow simulation show also the possibility of a reasonable reproduction or prediction of what occurs in the reality. Information required by the reviewer is provided further on
19. As the reviewer can appreciate the simulation is not perfectly symmetric/skew symmetric only in the very final stages of form filling, because of randomness of element distortion and remeshing-
20. As a matter of fact the plotted quantities are related to the simulated velocity field, which will be correlated to the nd surveyed orientation of the fibers. The modelling does not provide the orientation directly and so the authors decided in the logical process of showing and analyzing the results to proceed as done.
21. The figure has been commented. The red segments do represent the direction along which the maximum compensated inductance was calculated (it has been specified both in the text and in the figure caption)
22. Alfa and beta are indicators of the different figures (it is uncommon but cannot be prohibited) and should be clear from the figure captions. The first (c) has to be replaced by (b) and has been done.
23. Readability of figures improved

24. The scale of the colors is provide. Actually deviation from unit indicates, proportionally, the degree of higher or lower deviation from the nominal design content. Orientation is not meant to be read in these graphs; only local concentration. How this information can be used in the design is a matter of an ongoing study. The ambiguity of the title has been removed.
25. The results of the tests have been presented in another paper now published (for the sake of balance of paper length). The title has been changed and so the ambiguity claimed by the reviewer has been overcome. It is true that the goal of the ongoing study is to define an orthotropic constitutive law to be calibrated also as a function of fiber orientation.
26. Corrected, also accounting for the new figure numbering.
27. See above.
28. The sentence has been changed as follows:
    "a systematic agreement coincidence between the directions of the main cracks and those featuring the highest concentration and most favorable orientation of fibers is remarkablecan be observed".
    Comments provided in the subsequent paragraphs of the section
29. The issue of the slab with the 1/3 side defect has been commented. See response to reviewer 1.
30. Explanation added: *", highlighted by the sharpness and narrowness in color scale renderings".*
31. Yes. Figure numbers corrected, also taking into account new figure numbering.
32. Actually the curves provided by the authors are "iso-distribution" and "iso-concentration" ones.
33. It is true that the concept was not expressed in its best form
    The sentence has been modified as follows:
    "Fiber concentration/orientation patterns, as obtained from the ND-magnetic survey, and the crack patterns, observed on the slabs tested under center point load, matched satisfactorily, thus confirming the role of uneven fiber dispersion in governing the failure mode. The aforementioned comparison has also shown that dynamic segregation of fibers may represent sites for potential crack localization"
34. The holistic approach contains CFD and ND fiber monitoring. It has to be completed with structural design approaches based on orthotropic consitutive laws. Work is in progress. Ambiguity of the title has been removed.
    The whole paragraph has been modified as follows: *"This study showed the powerfulness of an holistic design approach which incorporated on CFD modeling and ND monitoring for structural elements made with highly flowable HPFRCCs, i.e., a tool for assessing the effect of fiber dispersion on the performance of hardened structural elements made of highly flowable HPFRCCs as affected by the tailored casting process. The approach has to be completed with the development of orthotropic constitutive laws for the material, which could be calibrated on the results obtained from CFD prediction and ND fiber survey."*

Highlights for review

Structural elements made with highly flowable UHPFRC: can Computational Fluid Dynamics (CFD) and non-destructive survey of fiber dispersion complement structural design in predicting failure modes?

Liberato Ferrara[1], *Massimiliano Cremonesi*[1], *Marco Faifer*[2], *Sergio Toscani*[2], *Luca Sorelli*[3], *Marc-Antoine Baril*[3], *Julien Réthoré*[4], *Florent Baby*[5], *François Toutlemonde*[5] *and Sébastien Bernardi*[6].

1. Combines different cutting edge techniques and methodologies for structural analysis and assessment of ultra high performance fibre reinforced concrete structures
2. Employs tailor made computational fluid dynamics tools for prediction of flow induced fiber orientation
3. Use tailor made non-destructive method for fiber dispersion and orientation assessment based on magnetic properties of fiber reinforced composites
4. Compares results from CFD modeling and ND fiber monitoring with structural failure patterns

Structural elements made with highly flowable UHPFRC: can Computational Fluid Dynamics (CFD) and non-destructive survey of fiber dispersion complement structural design in predicting failure modes?

Liberato Ferrara[1], *Massimiliano Cremonesi*[1], *Marco Faifer*[2], *Sergio Toscani*[2], *Luca Sorelli*[3], *Marc-Antoine Baril*[3], *Julien Réthoré*[4], *Florent Baby*[5], *François Toutlemonde*[5] *and Sébastien Bernardi*[6].

ABSTRACT

Structural design with highly flowable Fibre Reinforced Concrete has to duly take into account the preferential alignment of fibers, which can be governed through the rheological properties of the fluid mixture and the casting process and by the geometry of the structure. The possibility of predicting the fiber alignment, by tailoring the casting process, and of non-destructively monitoring it, can foster more efficient structural applications and design approaches.

Focusing on UHPFRC slabs with pre-arranged casting defects, the flow-induced alignment of the fibers has been predicted by means of a suitable CFD modelling approach and hence monitored via a non-destructive method based on magnetic inductance properties of the fiber reinforced composite. The comparison between the assessed data on the fibre orientation and the crack patterns as visualized by image analysis supports the effectiveness of casting flow modelling and non-destructive fiber dispersion monitoring in supporting the structural design of elements made with highly flowable fiber reinforced cementitious composites.

1 Politecnico di Milano, Department of Civil and Environmental Engineering, Milano, Italy
2 Politecnico di Milano, Department of Electronical Engineering and Bioengineering, Milano, Italy
3 Université Laval, Department of Water and Civil Engineering, Quebec, Canada
4 Institut National de Sciences Appliquées de Lyon, Lyon, France
5 IFSTTAR, Universitè Paris-Est, Marne la Vallée, France
6 Lafarge-Holcim, Paris, France

Structural elements made with highly flowable UHPFRC: correlating Computational Fluid Dynamics (CFD) predictions and non-destructive survey of fiber dispersion with failure modes

Liberato Ferrara[1], *Massimiliano Cremonesi*[1], *Marco Faifer*[2], *Sergio Toscani*[2], *Luca Sorelli*[3], *Marc-Antoine Baril*[3], *Julien Réthoré*[4], *Florent Baby*[5], *François Toutlemonde*[5] *and Sébastien Bernardi*[6].

1

ABSTRACT

Structural design with highly flowable Fibre Reinforced Concrete has to duly take into account the preferential alignment of fibers, which can be governed through the rheological properties of the fluid mixture and the casting process and by the geometry of the structure. The possibility of predicting the fiber alignment, by tailoring the casting process, and of non-destructively monitoring it, can foster more efficient structural applications and design approaches.

Focusing on UHPFRC slabs with pre-arranged casting defects, the flow-induced alignment of the fibers has been predicted by means of a suitable CFD modelling approach and hence monitored via a non-destructive method based on magnetic inductance properties of the fiber reinforced composite. The comparison between the assessed data on the fibre orientation and the crack patterns as visualized by image analysis supports the effectiveness of casting flow modelling and non-destructive fiber dispersion monitoring in supporting the structural design of elements made with highly flowable fiber reinforced cementitious composites.

1 Politecnico di Milano, Department of Civil and Environmental Engineering, Milano, Italy
2 Politecnico di Milano, Department of Electronical Engineering and Bioengineering, Milano, Italy
3 Université Laval, Department of Water and Civil Engineering, Quebec, Canada
4 Institut National de Sciences Appliquées de Lyon, Lyon, France
5 IFSTTAR, Universitè Paris-Est, Marne la Vallée, France
6 Lafarge-Holcim, Paris, France

1. Introduction

The advent of Ultra High Performance Fiber Reinforced Concrete and Cementitious Composites (UHPFRC, UHPFRCCs) on the construction market, a few decades ago, has paved the way for a novel approach to the concept and design of civil engineering structures and infrastructures.

On the one hand, the high deformation tolerance and energy dissipation capacity allows optimizing the dimensions of "conventional" structural elements (beam- and column-like) thanks to a more efficient structural use of the material. As a consequence, longer spans could be covered and higher load bearing capacity (or even larger lateral load resistance in the case of earthquake-resistant structures) could be achieved with reduced section dimensions, thus also reducing the self-supporting structural burden [1-3]. The enhanced performances in the hardened state are often associated with a superior performance in the fresh state. From the architectural point of view hence structural functions and complex shapes, which are hard to be cast with conventional reinforced concrete, can be easily obtained with UHPFRC [4-7].

In this framework, the dispersion of fibers inside a structural element, which is well recognized as a crucial issue in the reliability of structures made of Fiber Reinforced Concrete and Cementitious Composites plays a twofold role [8,9].

First of all a non-uniform dispersion of fibers, with zones with a reduced amount of fibers, may seriously affect the load bearing capacity as well as trigger unexpected failure mechanisms. Previous researches have pointed out that the non-uniform dispersion of fibers most likely occurs due to the negative effects of high fiber contents on the rheological properties of the fresh mixture [10,11]. A successful casting of conventional Fibre Reinforced Concrete (FRC) usually requires compaction and/or vibration, which may cause sedimentation of fibers, whereas contributing to an uneven spatial distribution of material mechanical properties inside the element.

Secondly, thanks to the synergistic effect with the superior fresh-state performance of UHPFRC, the need for manual compaction and vibration is reduced, resulting into a randomly uniform dispersion of fibers as well as into a more uniform spatial distribution of the material properties in the hardened state [12]. It has been furthermore shown that, thanks to both a suitably balanced set of fresh state properties and to a careful design of the casting process, it is possible to effectively orientate the fibers along the direction of the casting flow [13-15]. Both controlling and monitoring the fiber orientation during the casting process, is the first fundamental step towards a promising "holistic" approach to tailor the structural performance of UHPFRC structural elements. That is, enforcing the orientation of fibers along the direction of the principal tensile stress within the structural element when in service, will allow a more efficient structural use of the material to be effectively pursued [16-40]. Preferential orientation of fibers also jeopardize the isotropic material behavior assumption; the resulting even strongly orthotropic mechanical behavior of the material has to be duly taken into account in structural design, most of all when dealing with slab and shell structures which experience complex biaxial stress field arising from different load combinations.

The aforementioned "holistic design approach" for structures made with highly flowable FRC relies on two main "pillars" [41-42]. First, a reliable tool is needed, which predicts the alignment of the fibers by considering the rheological material properties and the casting process, including the geometry and boundary conditions of the structure to be cast; then, the assessment of the fiber distribution through a non-destructive time- and cost-effective method becomes a crucial quality control procedure.

2. Non-destructive monitoring of fiber dispersion

The early works on non-destructive monitoring of fiber dispersion in FRC structural elements employed X-ray imaging [43]. Besides the safety concerns related to the use of X-ray equipment on industrial scale, it is worth remarking that such methods, which have been also widely used thereafter by several researchers, mainly as a pre-check of destructive analyses [11] are able to provide an immediate visualization of the discrete fiber reinforcement network inside the analyzed region of the element, mainly in the case of steel fibers. As a matter of fact, the thickness of the element, in order to have meaningful information from the images, has to be necessarily limited, as a function of the power of the employed equipment and of the X-ray absorption capacity of the material. Furthermore, the unavoidable “loss” of the third dimension may introduce some artifacts in the results of image processing, affecting any quantitative information, e.g. about local fiber density, which could be garnered from it. The higher the fiber dosage and the aspect ratio of the fiber, the more influence have these artifacts.

Electrical methods, based on the effects of the fibers on the resistivity/conductivity of the composite material, have received lots of attention up to very recent years [44, 45]. Ozyurt et al. [46] employed the Alternate Current Impedance Spectroscopy (AC-IS) for the detection of fiber dispersion related issues and demonstrated its reliability as well as its sensitivity to fiber orientation, clumping, segregation etc. by means of extensive comparison with results obtained from destructive methods. Attempts were also made to address the application of the aforementioned method to industrial scale problems [47]. The method consists of applying to the specimen a voltage excitation over a wide range of frequencies (e.g. 10 MHz-1Hz) and measuring the amplitude and phase of the flowing current. When considering direct current (DC) or low frequency alternate current (AC), the behavior is practically insulating. However, the impedance Z significantly drops under high frequency alternate current excitation as a result of the displacement current. When the real and imaginary parts of the calculated impedance are plotted on a Nyquist diagram, FRCCs exhibit the so called dual-arc behavior, with two cusps, each of them represents a local minimum of the imaginary part of the impedance with respect to the real part. The rightmost cusp corresponds to the DC resistance across the electrodes, whose real part of the impedance R_m is essentially due to the matrix. Previous works have shown that it is weakly affected by the presence of the fibers. The leftmost, high frequency cusp is strictly related to the presence of conductive fibers in the matrix. It can be shown that the real part of the impedance R depends on the conductivity of the composite material. R_m and R can thus be used to estimate the concentration of the fibers by means of a simple mixture rule. In order to overcome the drawback of the sensitivity to moisture conditions, the so-called normalized resistivity is used:

$$\frac{R_m}{R} = 1 + [\sigma_{fibers}]V_f \quad (1)$$

where V_f is the fiber volume fraction and σ_{fibers} is the intrinsic conductivity of the fibers which, in the case of highly conductive fibers, only depends on their aspect ratio, which may affect the possibility to apply the method to the case of hybrid fiber reinforcement.

The method has been extensively employed to assess the influence of the fresh state performance on the dispersion and orientation of the fibers [12], clearly highlighting the better uniformity in fiber dispersion achievable through FR-SCC, together with a sensitivity to flow induced fiber alignment. Any direct quantitative comparison between, e.g., the concentration of fibers, as evaluated from Eq. (1) and data obtainable from destructive tests (e.g. crushing samples, separating and weighing fibers) could hardly be found in the literature. The need of a dedicated expensive instrumentation, required by the width of the employed frequency range, and the sensitivity of the method to the contact impedance between the surface electrodes and the structure surface, stand, so far, as the main hindrance to a wide application of the method at the industrial scale.

In order to overcome this problem, a method has been developed based on the evaluation of the equivalent capacitance between the electrodes of a probe which has to be simply laid on the surface of the structure under test. The technique allows assessing information about the average fiber concentration and their average direction. The measurement frequencies are relatively low (unto few hundreds of kilohertz) so that the required instrumentation is easily available and relatively inexpensive. However, the method suffers from high sensitivity to the humidity and to the coupling between the electrodes and the specimen.

Lataste et al. [48] employed a method based on low frequency resistance measurements, with a four electrode arrangement, aimed at reducing the effects of the poor electrical coupling. The method has been demonstrated to be effective in detecting orientation characteristics of the dispersed fiber reinforcement, because of the different resistance measured along the two directions at right angle to each other; a qualitative correlation with mechanical properties measured along the same directions as above was also provided [49, 50]. The method is by the way not able to provide any quantitative information about the local average concentration of the fibers. This is mainly due to the strong sensitivity of the concrete matrix resistivity to aging, moisture content and presence of electrolytes in the pores, which also affect the measured resistivity, beside the effect of fiber concentration.

The effects of conductive fibers on the dielectric properties of the fiber reinforced composite have led to the development of another method, based on the measurement of the effective permittivity through a coaxial probe and microwave reflectometry techniques [51]. Since the (known) fiber aspect ratio governs the capacitive behavior of the fibers and of the fiber reinforced composite, the local average concentration of fibers could be assessed by assuming a random fiber orientation. In view of this the method is not sensitive to a preferential alignment of the fibers.

Methods based on the study of heat transients and on the effect of fibers on the thermal diffusivity of the composite have been also tentatively applied for the non-destructive assessment of fiber concentration [52]. Temperature fields within a structural element can be easily surveyed through InfraRed (IR) thermography, but the slow propagation of temperature variations in thick members, which makes it difficult to provide a controlled input excitation over large areas, may limit the applicability of the method. More recently, a method based on micro-wave thermography has been developed and successfully applied to mortar specimens reinforced with different amounts of steel fibers [53].

X-ray Computed Tomography (CT) scans have been also widely employed in the last decade: as a matter of fact, they allow effective 3D visualization of the fiber network inside a FRC specimen [13, 39, 54-62], also in the case of non-conductive fibers [63], for which electrical methods cannot be applied. Limits on the specimen size and the need of an image analysis software for the quantitative processing of the collected data are so far the main concern in promoting the method for wider use, especially at the industrial scale.

Similar techniques, but employing SEM backscattered electron imaging, have been recently applied for the determination of the spatial dispersion of polymeric microfibers in strain hardening cementitious composites [64].

Methods, which employ a probe sensitive to the magnetic properties of the steel fibers have been recently proposed and validated [65-69]. In particular, the method proposed by Faifer et al. [70] , which has been employed in this work, relies on the fact that the steel fiber reinforced concrete is a mixture of two materials with very different magnetic permeability. The presence and the arrangement of the fibers modify the path of the magnetic field lines generated by the winding of a probe which results in a variation of its inductance. Fiber concentration can be quantitatively assessed by calibrating the method. Additionally the preferential orientation of the fibers can be estimated [71-72]. Besides its good sensitivity and robustness, the method also features an ease of use, due to a portable equipment, which just needs to be laid of the surface of a structural element, even sub-vertical ones, such as walls or slabs accessible only from the bottom, without any dedicated care about the coupling between the element free surface and the sensor. The authors also tested a twin coil probe with the attempt of investigating also the dissipative effects due to the alternating magnetic field which invests the steel fibers [70].

3 Numerical simulation of fresh concrete flow

The other "pillar" of the holistic design approach to structural applications made with highly flowable HPFRCCs is represented by the predictive modelling approach for both the fresh state behavior of the material and the casting process as a whole. This research topic, contrary to investigation on non-destructive monitoring of fiber dispersion, which dates back to about 40 years ago, has started attracting interest of scientists and practitioners only in the very last decade, once again triggered by the tremendous development in the field of Self Compacting/Highly Flowable Concrete and Cementitious Composites. Inspiration was drawn also from other fields of, *e.g.*, industrial engineering, with reference to processes such as metal forming and die casting, which, by analogy, also casts a light over the application of this field of research in advanced casting techniques such as 3D printing and additive manufacturing [73].

To the present state, numerical modelling of fresh concrete flow is employed as a tool for both:

- (i) understanding the correlation between rheological properties of fresh concrete and mix proportions, and hence improve the entire mix-proportioning approach,
- (ii) as well as for the simulation of the casting process as a whole, including predictions of particle migration, flow blockages and, in case, fiber orientation.

To this scope, Computational Fluid Dynamics (CFD) approaches are commonly employed, especially implementing (non-Newtonian) single fluid models for the description of the fresh concrete behavior and based on Galerkin FEM discretization of the Navier-Stokes equations, including free surfaces and moving boundaries [74, 75].

In order to describe the heterogeneous nature of FRC and its effect on flow-induced heterogeneity/anisotropy, Distinct Element Method (DEM) has been successfully employed [76-79].

The first theoretical basis of the fiber transport problem was laid down in the milestone work by Jeffery [80], who solved the moment equation of a rotating ellipsoid immersed in a Newtonian fluid. The fibers can be considered as infinitely elongated ellipsoid, and their interactions in a semi-dilute/concentrated suspension are suitably described by means of different approaches, among which the most common is the hydro-dynamically induced rotary diffusivity of isotropy [81, 82].

In this framework the evolution of a finite group of slender fibers with isotropic initial orientations is considered to represent the macroscopic orientation process. At each time step, the evolution of the orientation of each fiber is directly deduced from the Jeffery equation with the diffusive term of interactions, and the macroscopic orientation is then calculated as the mean of the orientation of all fibers. The number of chosen fibers is motivated by both a good accuracy of the prediction and the computation time. Applications of industrial interest have been addressed [15, 83, 84].

Ferrara et al. [85] and Ferrara and Cremonesi [86] have quite successfully attempted to correlate the orientation of the fibers to the direction of the shear rate vectors as predicted by the casting flow simulations. The same approach has been also followed by Orbe et al. [87] who also attempted to correlate the fiber orientation prediction in a full-scale casting geometry (a SFR-SCC wall) to the expectable spatial scattering of the material performance in the hardened state.

A fully coupled approach for the simulation of suspensions of non-Newtonian fluids and rigid particles has been recently proposed by employing the Lattice-Boltzmann method, with its roots in the kinetic theory of gases [88]. The approach treats fluids as individual particles discretized by a set of discrete particle distribution functions and provides rules for the mutual collisions and propagation. The coupled problem of the flow of suspensions of rigid bodies in a non-Newtonian fluid is separated into three levels:

i) level of particles, used for dynamics (position and velocities) and interactions of particles (collision and force);

ii) level of fluid-particles interaction with particles discretized by Lagrangian nodes and solved by the Immersed Boundary Method; and

iii) level of fluid, where the Lattice Boltzman Method is used for the flow modelling.

The macroscopic quantities can be then computed as moments of the distribution functions.

Successful application of this kind of approach to the simulation of SFR-SCC casting flows and prediction of flow-induced fiber orientation has been recently provided [73].

4. Research outline and significance

Within a comprehensive research effort aimed at developing a holistic approach to the control of execution of structural elements of highly flowable UHPFRC, this paper presents a real case study on HPFRCC slabs which have been cast with artificial flow-casting defects, *e.g.*, cold joints or other kinds of "in-structure" physical boundaries, which trigger a strong anisotropy and discontinuity in the flow-induced fiber orientation distribution.

The methodology consists on three steps: firstly, the casting process has been modeled by means of a Computational fluid Dynamics (CFD) modeling tool, employing a Lagrangian approach based on Particle Finite Element method [89, 90], and flow-induced orientation of fibers has been *"guessed"* through the velocity vector patterns of the simulated casting process .

Secondly, the fiber orientation has been then checked with a non-destructive method,which relies on the effect of the steel fibers on the magnetic properties of the FRCC.

Thirdly, a comprehensive correlation has been established with the cracking process and its development up to failure, as observed in the same slabs when tested under center point load in a suitable configuration (over 8 unilateral supports).

To the authors' knowledge, this work represents one of the first comprehensive throughout applications of the different predictive/monitoring approach with reference to UHPFRC elements. Moreover, it aims at showing how casting flow modeling and non-destructive survey of fiber dispersion can be usefully exploited as structural design aiding tools in assessing the reliability of anticipated failure modes in structural elements made with highly flowable FRCs, which may be quite sensitive to flow induced orientation of fibers.

5. Experimental program: materials, specimens, CFD prediction and ND fiber monitoring

A commercial UHPFRC (Ductal FM™) has been employed [91], containing 2% by volume of steel fibers, 13 mm long and with a diameter equal to about 0.2 mm and a yielding stress of 2860 MPa.

The UHPFRC was heat cured for 24 hours at 90°C and 100% RH; at 28 days it featured a compressive strength of 198.2 MPa and a Young's modulus equal to 58.2 GPa. The flexural behavior was also characterized by means of 4-Point Bending Tests (4PBT) on thin beam specimens, with dimensions of 420 mm x 110 mm x 30 mm (span x width x height) according to French recommendations [9].

Square 500 mm side and 30 mm thick slabs were cast, according to four different configurations:

(i) a slab without defect for which fresh concrete was poured from a corner, letting the flow fill the whole casing (Figure 1.a);

(ii) a slab with an aluminum divider placed at mid-side (Figure 1.b);

(iii) a slab with an aluminum divider placed at the side third, the fresh UHPFRC being poured, both in (ii) and (iii) from two opposite corners (Figures 1.c);

(iv) a slab with a diagonal divider, the fresh UHPFRC being poured from the other two opposite corners (Figure 1.d).

The aluminum divider was removed once the fresh concrete was fully cast in place, causing a strong discontinuity in the fiber distribution in the divider line, which may somehow represent a cold joint in real casting. Different colorants (brown and grey) were added to the mixtures, in order to distinguish the concrete cast from either corner.

The casting process of all the four investigated slabs was simulated with a Computational fluid Dynamics (CFD) model, employing a Lagrangian approach based on Particle Finite Element method, the detailed formulation of which has been described in [25,29]. The flow chart in Figure 2 summarizes the main steps of the approach. A re-meshing tool, based on maximum element distortion index, was implemented for an effective description of the free surface flow problem [90].

The employed HPFRCC has been modelled as a Bingham fluid with τ_0 = 20 Pa and μ = 100 Pas, as from previous investigations on the rheology of this kind of cementitious composites [92, 93].

Coherently with the approach adopted by the first author in [85], information about fiber orientation could be correlated to the direction of the flow velocity vectors in the simulated casting domain. This approach, though simplified, is able to provide the information about the trend of spatial orientation of fibers in the structural element as cast which may be sufficient for structural applications such as the ones herein dealt with. It is worth remarking that the benefits of fibers are best exploited in a structural configuration allowing for sufficient redistribution of post-cracking stresses, as the slabs here tested. In these cases "local" or "pointwise" information about fiber concentration and orientation may be redundantly detailed, since right the aforementioned stress redistribution capacity would allow to shadow concentrated defects, still remaining sensitive to a major "average spatial" trend in spatial dispersion and orientation of the fibers.

Non-destructive monitoring of fiber dispersion and orientation was performed on the slabs, once hardened, according to the methodology proposed in [71, 72], and hereafter briefly summarized

The employed set-up is shown in Figure 3, which consists of a C-shaped ferrite core with two windings: the first one generates the magnetic field, while the second is employed to pick up the induced electromotive force. The excitation winding is split into two coils which are wound around each leg of the probe. This arrangement is likely to increase the fraction of the magnetic flux linked with the coils which hits the material under test. The sense winding is placed over a coil of the excitation winding in order to reduce the leakage reactance. Figure 4 shows the flux density predicted by FEM magneto-static analysis. The measurement of the electromotive force induced in the pickup winding and of the current flowing through the excitation winding allows the losses due to the alternating magnetic field to be directly estimated. However, it is still not possible to separate the power losses due to the steel fibers from those due to the ferrite core. Under the assumption that the flux density in the core would not be affected by the presence of the steel fiber, the power losses due to steel fibers only could be estimated by evaluating the power losses when the probe is laid on the specimen and subtracting those measured when it is placed away from ferromagnetic objects. Nonetheless, since the ferromagnetic behavior of the steel fibers in the specimen increases the flux density in the core, the increase of the power losses due to the alternating magnetic field which is measured when the probe is placed on a SFRC specimen is only partially related directly to the losses occurring in the steel fibers, while the rest is caused by the increase of the core losses [71].

In order to avoid this problem, the sense winding has been employed to set up a proper feedback controller which imposes the voltage across it, hence its flux linkage. In this case the variation of the flux density in the ferrite core due to the steel fibers can be minimized, which furthermore results in minimized core losses. Thanks to the two-winding probe with a closed loop set-up, the difference between the losses due to the alternating magnetic field when the probe is placed on the specimen and those evaluated when it is placed away from any ferromagnetic material provides a good estimate of the power losses occurring in the steel fibers alone.

The measurement procedure is extremely simple: the probe is laid on the surface of the specimen, and the evaluation of the inductance is performed. Its value is clearly affected by both the fiber concentration and orientation in the specimen. The dependence on fiber concentration can be easily understood considering that the presence of steel fibers increases the effective magnetic permeability of the composite material according to a simple mixture rule, and, e.g., the impedance measured at the terminals of the equivalent electrical circuit can be expressed as:

$$Z = R_c + j\omega[L_1 + L_V] \quad (2)$$

where Rc denotes the resistance of the coil and L_l and Lv respectively denote the magnetic inductance associate to a magnetic flux outside and through the specimen. The inductance Lv can be split into a matrix contribution L_{v0} and an incremental contribution $\Delta L_{v,fibers}$, denoted as compensated inductance henceforth, which depends on the fiber volume fraction and orientation. Whereas inductance Lv depends on the measurement frequency, compensated inductances results independent of it [70-72].

The procedure to assess the effect of the fiber orientation has to take into account that the electromagnetic properties of the composites, as remarked above, become anisotropic (dyadic) if the fibers are not randomly oriented. In case of a preferential alignment of the fibers, by rotating the probe on the specimen and measuring the inductance along different directions, a dependence of the measured inductance on the probe orientation will be detected: the direction along which the maximum value of the inductance is measured will most likely coincide with the preferential alignment of the fibers. The magnitude of the inductance variation is correlated to the degree of orientation of the fibers.

The UHPFRC slabs were analyzed according to different “cell-schematics” as shown in Figure 5, measurements in each cell being taken along four different directions, namely at 0°, 45°, 90° and 135° to a reference y-axis. For each direction measurements were repeated four times, and reference will be made henceforth to the average of the four thus garnered values. Arrows in Figure 5 indicate the direction of casting, whereas the solid thicker line indicates the pre-arranged discontinuity. The choice of the measuring grids was dictated by the geometry of the slab and by the position of the casting defect, as well as by the need of garnering information on fiber dispersion and orientation also across the same casting defects as above.

Quantitative assessment of local concentration of fibers, for each of the measured slab cells, was performed through the calibration of the relationship between the "nominal average compensated inductance" and the nominal "design" fiber content in the mix. The former is defined as the average, computed over the whole slab, of the averages of the compensated inductance as measured along the four directions for each cell. By means of such a calibrated law, the average values of compensated inductance for each cell could be processed to assess whether and to what extent the local concentration of fibers differed from the assumed nominal value. For the assessment of fiber orientation, "fractional" compensated inductances along each direction α were calculated as:

$$f_\alpha = \frac{\Delta L_\alpha}{0.25\left(\Delta L_0 + \Delta L_{45} + \Delta L_{90} + \Delta L_{135}\right)} \qquad (3).$$

6. Casting flow simulations

Figures 6 a-d show some significant snapshots of the simulated casting processes for all the four investigated slabs. The iso-velocity lines for advancing flow front along the simulated flow processes as well as the velocity field vectors were obtained, as shown in Figures 7 a-d and 7 e-h respectively. The envelope lines represent the advancement of the fluid front along the casting process, transporting and aligning the immersed fibers. They are going to be correlated to the orientation of the fibers, as assessed through the non-destructive magnetic survey in the forthcoming section.

7. Non-destructive magnetic surveyed fiber dispersion and orientation

As preliminary information obtainable from the non-destructive survey of fiber dispersion and orientation, the directions have been plotted (Figures 8 a-d) along which the maximum values of compensated inductances have been measured (as from the schematics in Figure 5). The aforementioned directions (red segments in Figure 8) do correspond fairly well to the computed flow streamlines which model the advancement of the free flow front in the simulated casting process. This is also in agreement with previous literature findings, for which in a free casting flow fibers tend to align parallel to the free edges of the same flow [31, 49, 79].

In Figures 9 a-d, polar plots of the fractional compensated inductances allow to have a deeper insight into the degree of anisotropy in fiber dispersion, caused by the casting flow process as by the prearranged geometrical discontinuities, in case. As a matter of fact the fractional compensated inductance represents a measure of how much the inductance measured along one direction exceeds the average isotropic value and hence is an effective measure of the fiber dispersion anisotropy.

It can be observed that in the reference slab without any geometrical discontinuity a substantially isotropic dispersion has been obtained, with some moderate deviations most likely due to wall effects along the boundaries. On the other hand, in the slabs with a geometrical discontinuity, either parallel to the side or diagonally arranged, the fiber dispersion features evident anisotropy because of the wall effect provided by the discontinuity. Interestingly the anisotropy is better detected when the sensor is placed across the discontinuity (Figures 9 a-d)

Figures 10 a-d provide information about local fiber concentration, in the form of "iso-quantity" curves, as explained in detail in section 3. Such quantitative information is obtained by calculating the average value of the four measurements garnered in each single cell and normalizing it by the average of the averages, referring to the structural element as a whole. The latter quantity can be regarded as an indicator of the nominal content of fibers inside the structural element. Zones where the value of such a normalized local average compensated inductance is higher than one thus will indicate zones with potentially higher local concentration of fibers.

From plots in Figures 10 a-d, the following observations can be drawn:

- the degree of homogeneity of fiber concentration inside each single slab is quite good, observed deviations always falling in the range ± 10-15%;
- in the reference slab, diagonally cast from one single corner and with no geometrical

discontinuity inside, the aforementioned heterogeneity is evidently due to dynamic segregation of the fibers along the casting direction, as well as to some corner effects;

- in the slabs with prearranged defects, the effect of dynamic segregation of the fibers is less strong, most likely because of the lower distance travelled by the casting flow. On the other hand a sensible difference between the two "halves" of the slab appear: the half which was cast as the former being always poorer, in fiber content, than the latter, which was cast only once the former was completed. This fact can be justified by invoking some static segregation which may have occurred in the bucket employed to cast the slabs, which made richer in fibers the portion of the bulk material which was poured later in the molds.

Information about local fiber concentration and orientation has been jointly plotted in Figures 12 a-d, where the local compensated inductances, along each of the four surveyed directions in each cell, have been weighed by the concentration homogeneity factor, as above in Figures 10 a-d. This allows having an output of immediate graphical significance, which indicates in a clear way where a larger concentration of fibers could be expected and along which direction.

8. Comparison between fiber dispersion patterns and crack patterns

As a final check, which also stands as a proof of the significance of the whole performed investigation, a comparison has been attempted between the fiber dispersion patterns, as in Figures 10 a-d, and the cracking patterns obtained when testing the same surveyed slabs under center point load, according to the schematic set-up shown in Figure 11.

Crack patterns have been surveyed by means of a dedicated Digital Image Correlation (DIC) set-up and system, described in detail in [91, 94], where also information about the results of mechanical tests can be found.

Crack patterns, as evolving along the loading path and up to failure, are shown in Figures 13 a-d, and superimposed to fiber concentration and orientation patterns in Figures 14 a-d.

Besides the clear influence of the prearranged discontinuity, at least in two of the three investigated cases featuring it, a systematic agreement between the directions of the main cracks and those featuring the highest concentration and most favorable orientation of fibers can be observed. That is, the cracks formed orthogonally to the direction of weakest post-cracking performance of the material, which is that of least favorable orientation of the fibers. Moreover, and quite more interestingly, front of dynamic segregation, i.e. zones in the slab where a steeper decrease in local fiber concentration was observed, highlighted by the sharpness and narrowness in color scale renderings, also acted both as a defect and as an arresting front for the cracks, which hence tended to propagate parallel to it.

This is evident in the case of the reference slab with no defect, where fibers dispersion was quite isotropic as only slightly affected by some degree of dynamic segregation of the same fibers starting from the casting corner. The main cracks evidently developed following, as above said, with the front of dynamic segregation (Figure 13 a). With reference with the slab with the casting defect at 1/3 of the side the evidence of the casting defect on failure mode is less immediate. As a matter of fact, though the major crack did not followed the casting defect boundary, the presence of the last only allowed one major longitudinal crack to localize. Moreover the radial micro-cracks developed asymmetrically, with clear evidence of the zone where larger concentration of fibers was detected and where larger post-cracking stress redistribution was allowed.

The matching between weak crack plane and the measured fibre orientation confirms thus the reliability of the non-destructive fiber dispersion monitoring approach.

This highlights once again the importance of coherently "incorporating" flow-induced orientation of the fibers in the structural design of elements made with highly flowable HPFRCCs. This can be accomplished either through a "one-parameter" approach, such as the K-factor one proposed by *fib* Model Code 2010 [8,9] or with advanced approaches which make explicit reference to an "in-structure monitored" orientation of the fibers. The latter, on its hand, can be accounted for in a deterministic way, with reference only to the main fiber alignment, as this study would pave the way for, as well as through more refined probabilistic fiber orientation distributions [39, 40].

9. Concluding remarks

The coherence between the presented results in term of magnetic inductance, simulated fiber orientation and crack patterns as measured using digital image correlation corroborate the reliability of the proposed approach. It also confirms that a single fluid approach can be reasonably employed to the aforementioned purpose, i.e., fiber alignment being predictable via the modeled field of the shear rate vector. Furthermore, the combined analyses have coherently confirmed flow-induced orientations of fibers in free casting flows.

Fiber concentration/orientation patterns, as obtained from the ND-magnetic survey, and crack patterns, observed on the slabs tested under center point load, matched satisfactorily, thus confirming the role of uneven fiber dispersion in governing the failure mode The aforementioned comparison has also shown that dynamic segregation of fibers may represent sites for potential crack localization.

This study showed the powerfulness of a holistic design approach which incorporated on CFD modeling and ND monitoring for structural elements made with highly flowable HPFRCCs, i.e., a tool for assessing the effect of fiber dispersion on the performance of hardened structural elements made of highly flowable HPFRCCs as affected by the tailored casting process. The approach has to be completed with the development of orthotropic constitutive laws for the material, which could be calibrated on the results obtained from CFD prediction and ND fiber survey. This opens the possibility of not only predicting but also optimizing casting flow process of highly flowable HPFRCCs with respect to the structural applications.

Acknowledgements

The authors acknowledge the financial support of the National Sciences and Engineering Research Council of Canada (NSERC) funding - Collaborative Research and Development Grants (RDCPJ 445200). The authors are also grateful to Mr. Gabriele Mero and Mr. Gregorio Nicol Villirillo, who

performed the non-destructive survey of fibre dispersion, in partial fulfilment of the requirements for the achievement of their BEng in Civil Engineering at Politecnico di Milano.

References

[1] Kunieda, M. and Rokugo, K. (2006), "Recent progress on HPFRCC in Japan: required performance and applications", *Journal of Advanced Concrete Technology*, 4 (1), pp. 19-33.

[2] Graybeal, B. (2006), “Structural Behavior of Ultra-High Performance Concrete Prestressed I-Girders,” FHWA-HRT-06-115, U.S. Department of Transportation, Federal Highway Administration, Washington, DC, 104 pp.

[3] Graybeal, B. (2009), “Structural Behavior of a Prototype Ultra-High Performance Concrete Pi-Girder,” NTIS Report No. PB2009-115495, U.S. Department of Transportation, Federal Highway Administration, Washington, DC, 145 pp.

[4] Aïtcin, P. C., Lachemi, M., Adeline, R. and Richard, P. (1998), “The Sherbrooke reactive powder concrete footbridge”, *Structural Engineering International*, 2 (8).

[5] Vicenzino, E., Culham, G., Perry, V.H., Zakariasen, D and Chow, T.S. (2005), “First use of UHPFRC in thin precast concrete roof shell for Canadian LRT station”, *PCI Journal*, Sept-Oct issue, pp. 50-67.

[6] Walraven, J. (2009), “High Performance Fiber Reinforced Concrete: Progress in Knowledge and Design Codes”, *Materials and Structures*, 42, pp. 1247-1260.

[7] Sorelli, L. and Toutlemonde, F. (2005), “Finite element modelling of FRC/UHPFRC in support of innovative structural applications, In: Proceedings of the 3rd International Conference on Costruction Materials: Performance, Innovations and structural implications, CONMAT-05, Vancouver, Canada, August 22-24, 2005.

[8] *fib* Model Code 2010, 2012, 2 volumes.

[9] Toutlemonde, F. and Resplendino, J., eds. (2012), “Designing and Building with UHPFRC: State of the Art and Development” ISBN: 978-1-84821-271-8, hardcover, *Wiley-ISTE*,

London-New York, 814 pp..

[10] Bayasi, M.Z. and Soroushian, P. (1992), "Effect of steel fiber reinforcement on fresh mix properties of concrete", *ACI Materials Journal*, 89 (2), pp. 369-374.

[11] Ferrara, L. and Meda, A. (2006), "Relationships between fibre distribution, workability and the mechanical properties of SFRC applied to precast roof elements", *Materials and Structures*, 39 (4), pp. 411-420.

[12] Ferrara, L., Park, Y.D. and Shah, S.P. (2008), "Correlation among fresh state behaviour, fiber dispersion and toughness properties of SFRCs", *ASCE Journal of Materials in Civil Engineering*, 20 (7), pp. 493-501.

[13] Stahli, P., Custer, R. and van Mier, J.G.M. (2008), "On flow properties, fibre distribution, fibre orientation and flexural behaviour of FRC". *Materials and Structures*, 41 (1), pp. 189-196.

[14] Ferrara, L., Ozyurt, N. and di Prisco, M. (2011), "High mechanical performance of fiber reinforced cementitious composites: the role of "casting-flow" induced fiber orientation", *Materials and Structures*. 44 (1), pp. 149-168.

[15] Martinie, L. and Roussel N. (2010), "Simple tools for fiber orientation prediction in industrial practice", *Cement and Concrete Research*, 41, pp. 993-1000.

[16] Toutlemonde F., Sercombe J., Torrenti J.M. and Adeline R. (1999), "Développement d'un conteneur pour l'entreposage de déchets nucléaires : résistance au choc", *Revue Française de Génie Civil*, 3 (7-8), pp. 729-756.

[17] Grunewald, S. (2004), "Performance based design of self compacting steel fiber reinforced concrete", PhD Thesis, Delft University of Technology.

[18] Toutlemonde, F. (2004), "Contribution à la connaissance et à la maîtrise de quelques non-linéarités du comportement mécanique des bétons et de leur effet sur le fonctionnement des structures, assortie de quelques réflexions méthodologiques", *Etudes et recherches des LPC*, OA42.

[19] Ferrara, L., Faifer, M., Muhaxheri, M. and Toscani, S. (2012), "A magnetic method for non destructive monitoring of fiber dispersion and orientation in Steel Fiber Reinforced Cementitious Composites – part 2: correlation to tensile fracture toughness", *Materials and Structures*, 45 (4), pp. 591-598.

[20] Orbe, A., Cuadrado, J., Losada R. and Rojì, E., (2012) "Framework for the design and analysis of steel fiber reinforced self-compacting concrete structures", *Construction and Building Materials*, 35, pp. 676-686.

[21] Ferrara, L., Bamonte, P., Caverzan, A., Musa, A. and Sanal, I. (2012), "A comprehensive methodology to test the performance of Steel Fibre Reinforced Self-Compacting Concrete (SFR-SCC)", *Construction and Building Materials*, 37, pp. 406-424.

[22] Abrishambaf, A., Barros, J.A.O. and Cunha, V.M.C.F. (2013), "Relation between fibre distribution and post-cracking behaviour in steel fibre reinforced self-compacting concrete panels", *Cement and Concrete Research*, 51, pp. 57-66.

[23] di Prisco, M., Ferrara, L. and Lamperti, M.G.L. (2013), "Double Edge Wedge Splitting (DEWS): an indirect tension test to identify post-cracking behaviour of fibre reinforced cementitious composites", *Materials and Structures*, 46 (11), pp. 1893-1918.

[24] Sanal, I. and Ozyurt Zihnioğlu, N. (2013), "To what extent does the fiber orientation affect mechanical performance?", *Construction and Building Materials*, 44, pp. 671-681.

[25] Orbe, A., Rojì, E., Losada R. and Cuadrado, J.,(2014), "Calibration patterns for predicting residual strengths of steel fibre reinforced concrete (SFRC)", *Composites – Part B: Engineering*, 58, pp. 408-417.

[26] Pujadas, P., Blanco, A., de la Fuente, A., Cavalaro, S.H.P. and Aguado, A. (2014), "Multidirectional double punch test to assess the post-cracking behaviour and fibre orientation of FRC", *Construction and Building Materials*, 58, pp. 214-224.

[27] Pujadas, P., Blanco, A., de la Fuente, A., Cavalaro, S.H.P. and Aguado, A. (2014), "Fibre distribution in macro-plastic fibre reinforced concrete slab-panels", *Construction and*

Building Materials, 64, pp. 496-503.

[28] Švec, O., Žirgulis, G., Bolander, J.E. and Stang, H. (2014), "Influence of formwork surface on the orientation of steel fibres within self-compacting concrete and on the mechanical properties of cast structural elements", *Cement and Concrete Composites*, 50, pp. 60.72.

[29] Xia, J. and Mackie, K. (2014), "Axisymmetric Fiber Orientation Distribution of Short Straight Fiber in Fiber-Reinforced Concrete", *ACI Materials Journal*, 111 (2), pp. 133-142.

[30] Yoo, D.Y., Kang, S.T. and Yoon, Y.S. (2014), "Effect of fiber length and placement method on flexural behavior, tension-softening curve, and fiber distribution characteristics of UHPFRC", *Construction and Building Materials*, 64, pp. 67-81.

[31] Abrishambaf, A., Barros, J.A.O. and Cunha, V.M.C.F. (2015), "Tensile stress–crack width law for steel fibre reinforced self-compacting concrete obtained from indirect (splitting) tensile tests", *Cement and Concrete Composites*, 57, pp. 153-165.

[32] Blanco, A., Pujadas, P., de la Fuente, A., Cavalaro, S.H.P. and Aguado, A. (2015), "Assessment of the fibre orientation factor in SFRC slabs", *Composites – Part B: Engineering*, 68, pp. 343-354.

[33] Ferrara, L. (2015), "Tailoring the orientation of fibers in High Performance Fiber Reinforced Cementitious Composites: part 2 - correlation to mechanical properties and design implications", *Journal of Materials and Structures Integrity*, 9 (1/2/3), pp. 92-107.

[34] Lameiras, R., Barros, J.A.O., Azenhab, M. (2015), "Influence of casting condition on the anisotropy of the fracture properties of Steel Fibre Reinforced Self-Compacting Concrete (SFRSCC)", *Cement and Concrete Composites*, 59, pp. 60-76.

[35] Yoo, D.Y., Zi, G., Kang, S.T. and Yoon, Y.S. (2015), "Biaxial flexural behavior of ultra-high-performance fiber-reinforced concrete with different fiber lengths and placement methods", *Cement and Concrete Composites*, 63, pp. 51-66.

[36] Bastien-Masse, M., Denarié, E. and Brühwiler, E. (2016), "Effect of fiber orientation on the in-plane tensile response of UHPFRC reinforcement layers", *Cement and Concrete*

Composites, 67, pp. 111-125.

[37] Sarmiento, E.V., Geiker, M. and Kanstad, T. (2016), "Influence of fibre distribution and orientation on the flexural behaviour of beams cast from flowable hybrid polymer–steel FRC", *Construction and Building Materials*, 109, pp. 166-176.

[38] Žirgulis, G., Śvec, O., Geiker, M., Cwirzen A. and Kanstad, T. (2016), "Variation in fibre volume and orientation in walls: Experimental and numerical investigation", *Structural Concrete*, DOI: 10.1002/suco.201500060.

[39] Žirgulis, G., Śvec, O., Geiker, M., Cwirzen A. and Kanstad, T. (2016), "Influence of reinforcement bar layout on fibre orientation and distribution in slabs cast from fibre-reinforced self-compacting concrete (FRSCC)", *Structural Concrete*, DOI: 10.1002/suco.201500064.

[40] Guenet T. (2016), "Modélisation du comportement des bétons fibrés à ultra-hautes performances par la micromécanique : effet de l'orientation des fibres à l'échelle de la structure", PhD thesis, Thèse en cotutelle Université Laval - Université Paris-Est, 31 mars 2016, 322 pp.

[41] Laranjeira, F., Grünewald, S., Walraven, J., Blom, C., Molins, C. and Aguado, A. (2011), "Characterization of the orientation profile of steel fiber reinforced concrete", *Materials and Structures*, 44 (6), pp. 1093-1111.

[42] Laranjeira F., Aguado, A., Molins, C., Grünewald, S., Walraven, J. and Cavalaro, S.H.P. (2012), "Framework to predict the orientation of fibers in FRC: a novel philosophy", *Cement and Concrete Research*, 42, pp. 752-768.

[43] Stroeven, P. and Shah, S.P. (1978), "Use of radiography-image analysis for steel fiber reinforced concrete". In: Swamy, R.N. (ed.) Testing and test Methods of Fiber Cement Composites, Construction Press, Lancaster: 345-353.

[44] Woo, L. Y., Wansom, S., Ozyurt, N., Mu, B, Shah, S. P., and Mason, T. O. (2005), "Characterizing fiber dispersion in cement composites using AC Impedance Spectrometry",

Cement and Concrete Composites, 27, pp. 627-636.

[45] Eik, M., Lohmus, K., Tigasson, M., Listan, M., Puttonen, J. and Herrmann, H. (2013), "DC-conductivity testing combined with photometry for measuring fiber orientations in SFRCs", *Journal of Materials Science*, 48 (10), pp. 3745-3759.

[46] Ozyurt, N., Woo, L.Y., Mason, T.O. and Shah, S.P. (2006), "Monitoring fiber dispersion in fiber reinforced cementitious materials: comparison of AC Impedance Spectroscopy and Image Analysis". *ACI Materials Journal*, 103 (5), pp. 340-347.

[47] Ozyurt, N., Mason, T.O. and Shah, S.P. (2006), "Non destructive monitoring of fiber orientation using AC-IS: an industrial scale application", *Cement and Concrete Research*, 36, pp. 1653-1660.

[48] Lataste, J.F., Behloul M. and Breysse, D. (2008), "Characterisation of fibres distribution in a steel fibre reinforced concrete with electrical resistivity measurements", *Non Destructive Testing and Engineering International*, 41 (8), pp. 638-647.

[49] Barnett, S., Lataste, J.F., Parry, T., Millard, S. G. and Soutsos, M.N. (2010), "Assessment of fibre orientation in ultra high performance fiber reinforced concrete and its effect on flexural strength", *Materials and Structures*, 43 (7), pp. 1009-1023.

[50] Lataste, J.F., Barnett, S.J., Parry, T. and Tsoutsos, M.N. (2011), "Study of fiber distribution and orientations in UHPFRC by electrical resistivity and mechanical tests", *European Journal of Environmental and Civil Engineering*, 15 (4), pp. 533-544.

[51] Van Damme, S., Franchois, A., De Zutter, D. and Taerwe, L. (2009), "Nondestructive determination of the steel fiber content in concrete slabs with an open-ended coaxial probe", *IEEE Transactions on Geoscience and Remote Sensing*, 42 (11), pp. 2511 –2521.

[52] Felicetti, R. and Ferrara L. (2008), "The effect of steel fibre on concrete conductivity and its connection to on-site material assessment", Proceedings of Befib 2008, 7th International RILEM Symposium on Fiber Reinforced Concrete, R. Gettu ed., Chennai, India, 17-19 September 2008, RILEM Pubs., pp. 525-536.

[53] Foudazi, A., Mehdipour, I., Donnel, K.M. and Khayat, K.H. (2016), “Evaluation of steel fiber distribution in cement based mortars using active microwave thermography”, *Materials and Structures*, DOI 10.1617/s11527-016-0843-3.

[54] Liu, J., Li, C., Liu, J., Cui, G. and Yang, Z. (2013), “Study on 3D spatial distribution of steel fibers in fiber reinforced cementious composites through micro CT scans”, *Construction and Building Materials*, 48, pp. 656-661.

[55] Suuronen, J.P., Kallonen, A:, Eik, M., Puttonen, J., Serineaa, R. and Herrmann, H. (2013), “Analysis of short fibers orientation in steel fiber reinforced concrete (SFRC) by X-ray tomography”, *Journal of Materials Science*, 48, pp. 1358-1367.

[56] Vicente, M.A., Gonzalez, D.C. and Maynez, J. (2014), “Determination of dominant fibre orientations in fibre reinforced high strength concrete elements based on computed tomography scans”, *Non Destructive Testing and Evaluation*, 29 (2), pp. 164-182.

[57] Zofka, A:, Paliukaiti, M., Vaitkus, A., Maliszewski, D., Josku, R. and Bernier, A. (2014), “Laboratory study on the influence of casting on properties of ultra-high performance fiber reinforced concrete (UHPFRC) specimens”, *Journal of Civil Engineering and Management*, 20 (3), pp. 380-388.

[58] Ponikiewski, T., Katzer, J., Bugdol, M. and Rudzki, M. (2015), “Steel fiber spacing in self-compacting concrete precast walls by X-ray computed tomography”, *Materials and Structures*, 48, pp. 3863-3874.

[59] Ponikiewski, T., Golaszewski, J., Rudzki, M. and Bugdol, M. (2015), “Determination of steel fibers distribution in self-compacting concrete beams using X-ray computed tomography”, *Archives of Civil and Mechanical Engineering*, 15 (2), pp. 558-568.

[60] Ponikiewski, T., Katzer, J., Bugdol, M. and Rudzki, M. (2015), “X-ray computed tomography harnessed to determine 3D spacing of steel fibers in self-compacting concrete (SCC) slabs”, *Construction and Building Materials*, 74, pp. 102-108.

[61] Herrmann, H., Pastorelli, E., Kallonen, A. and Suuronen, J.P. (2016), "Methods for fibre orientation analysis of X-ray tomography images of steel fibre reinforced concrete (SFRC)", *Journal of Materials Science*, 51 (8), pp. 3772-3783.

[62] Ponikiewski, T. and Katzer, J. (2016), "X-ray computed tomography of fiber reinforced self-compacting concrete as a tool of assessing its flexural behavior", *Materials and Structures*, DOI 10.1617/s1527-015-0638y.

[63] Bordelon, A.C. and Roesler, J.R. (2014), "Spatial distribution of synthetic fibers in concrete with X-ray computed tomography", *Cement and Concrete Composites*, 53, pp. 35-43.

[64] Felekoglu, B., Tomer-Felekoglu, K. and Göden, E. (2015), "A novel method for the determination of polymer micro-fiber distribution of cementitious composites exhibiting multiple cracking behavior under tensile loading", *Construction and Building Materials*, 86, pp. 95-94.

[65] Faifer, M., Ottoboni, R., Toscani, S., Ferrara, L. (2011). "Non-destructive Testing of Steel Fiber Reinforced Concrete using a Magnetic Approach", *IEEE Transactions on Instrumentation and Measurement*, 60 (5), pp. 1709-1717.

[66] Torrents, J.M., Blanco, A., Pujadas, P., Aguado, A., Juan-Garcia, P., Sanchez-Moraguez, M.A. (2012), "Inductive method for assessing the amount and orientation of steel fibers in concrete", *Materials and Structures*, 45 (10), pp. 1577-1592.

[67] Al-Mattarneh, H. (2014), "Electromagnetic quality control of steel fibre concrete", *Construction and Building Materials*, 73, pp. 350-356.

[68] Cavalaro, S.H.P., Lopez, R., Torrents, J.M. and Aguado, A. (2015), "Improved assessment of fiber content and orientation with inductive method in SFRC", *Materials and Structures*, 48 (6), pp. 1859-1873.

[69] Cavalaro, S.H.P., Lopez-Carreño, R., Torrents, J.M., Aguado, A. and Juan-Garcia, P. (2016), "Assessment of fibre content and 3D profile in cylindrical SFRC specimens", *Materials and Structures*, 49 (1), pp. 577-595.

[70] Faifer, M., Ferrara, L., Ottoboni, R. and Toscani, S. (2013), “Low frequency electrical and magnetic methods for non-destructive monitoring of fiber dispersion in fiber reinforced cementitious composites: an overview”, *Sensors*, 13, pp. 1300-1318.

[71] Ferrara, L., Faifer, M. and Toscani, S. (2012), “A magnetic method for non destructive monitoring of fiber dispersion and orientation in Steel Fiber Reinforced Cementitious Composites – part 1: method calibration”, *Materials and Structures*, 45 (4), pp. 575-589.

[72] Ferrara, L., Faifer, M., Muhaxheri, M. and Toscani, S. (2012), “A magnetic method for non destructive monitoring of fiber dispersion and orientation in Steel Fiber Reinforced Cementitious Composites – part 2: correlation to tensile fracture toughness”, *Materials and Structures*, 45 (4), pp. 591-598.

[73] Simulation of Fresh Concrete Flow. State of the Art Report of the RILEM Technical Committee 222-SCF, N. Roussel and A. Gram, eds., Springer, 2014, ISBN 978-94-017-8883-0, 147 pp.

[74] Roussel, N., Geiker, M., Dufour, F., Thrane, L.N. and Szabo, P (2007), “Computational modeling of concrete flow: general overview”, *Cement and Concrete Research*, 37, pp. 1298-1307.

[75] Roussel, N., Gram, A., Cremonesi, M., Ferrara, L., Krenzer, K., Mechtcherine, V., Shyshko, S., Skocek, J., Spangenberg, J., Svec, O., Thrane, L.N. and Vasilic, K. (2016), “Numerical simulations of concrete flow: a benchmark comparison”, *Cement and Concrete Research*, 69, pp. 265-271.

[76] Mechtcherine, V., Gram, A., Krenzer, K., Schwabe, J.-H., Shyshko, S., Roussel N. (2014), “Simulation of fresh concrete flow using DEM: theory and applications”, *Materials and Structures*, 47, pp. 615–630.

[77] Shyshko, S., Mechtcherine, V. (2013), “Developing a Discrete Element Model for simulating fresh concrete: experimental investigation and modelling of interactions between discrete aggregate particles with fine mortar between them”, *Construction and Building*

Materials, 47, pp. 601-615.

[78] Mechtcherine, V., Shyshko, S. (2015), “Simulating the behaviour of fresh concrete with the Distinct Element Method – Deriving model parameters related to the yield stress”, *Cement and Concrete Composites*, 55, pp. 81–90.

[79] Ferrara, L., Shyshko, S., Mechtcherine, V. (2012), “Predicting the flow-induced dispersion and orientation of steel fibers in SCC by DEM”, in J. Barros et al. eds., Proceedings BEFIB 2012, Guimaraes, Portugal, September 20-22, 2012, RILEM Pubs., 12 pp.

[80] Jeffery, G.B. (1923), “The motion of ellipsoidal particles immersed in a viscous fluid,” *Proceedings of the Royal Society of London A*, vol. 102, pp. 161–179.

[81] Folgar, F. and Tucker III, C.F., (1984), “Orientation behavior of fibers in concentrated suspensions”, *Journal of Reinforced Plastics and Composites*, 3, pp. 98–119.

[82] Advani, S.G. and C.F. Tucker III, (1987), “The use of tensors to describe and predict fiber orientation in short fiber composites,” *Journal of Rheology*, 31 (8), pp. 751–784, 1987.

[83] Dupont D. and Vandewalle, L. (2005), “Distribution of steel fibres in rectangular sections”. *Cement and Concrete Composites*, 27, pp. 391–398

[84] Martinie, L., Lataste, J.F. and Roussel, N. (2015), “Fiber orientation during casting of UHPFRCC: electrical resistivity measurements, image analysis and numerical simulations”, *Materials and Structures*, 48 (4), pp. 947-957.

[85] Ferrara, L., Tregger, N. and Shah, S.P. (2010), “Flow-induced fiber orientation in SCSFRC: monitoring and prediction”, in Proceedings SCC2010, K.H. Khayat and D. Feys eds., 2010, Montreal, Canada, Springer, pp. 417-428.

[86] Ferrara, L., Cremonesi, M.: “Effects of casting process on toughness properties of Fiber Reinforced-Self Compacting Concrete as from EN 14651”, in N. Roussel and H. Bessaies-Bey, eds., Proceedings 7th RILEM International Conference on Self Compacting Concrete and 1st RILEM International Conference on Rheology and Processing of Construction Materials, Paris, France, 1-3 September 2013, CD-Rom.

[87] Orbe, A., Losada, R., Roji, E. and Cuadrado, J. (2014), "The prediction of bending strengths in SFRSCC using Computational Fluid Dynamics (CFD)", *Construction and Building Materials*, 66, pp. 587-596.

[88] Svec, O. (2013), "Flow modelling of steel fibre reinforced self-compacting concrete", *PhD Thesis*, Technical University of Denmark.

[89] Cremonesi, M., Frangi, A. and Perego, U. (2010), "A Lagrangian finite element approach for the analysis of fluid–structure interaction problems", *International Journal for Numerical Methods in Engineering*, 84 (10), pp. 610-630.

[90] Cremonesi, M., Ferrara, L., Frangi, A., and Perego, U. (2010), "Simulation of the flow of fresh cementitious suspensions by a Lagrangian Finite Element approach", *Journal of Non-Netwonian Fluid Mechanics*, 165, pp. 1555-1563.

[91] Baril, M. (2016), "Effet de défauts de coulage sur la micro-fissuration des dalles minces en béton fibre à ultra-hautes performances par stéréovision et corrélation d'images digitales", Master Thesis, Université Laval, Avril 2016.

[92] Ferrara, L., Cremonesi, M., Tregger, N., Frangi, A. and Shah, S.P. (2012), "On the identification of rheological properties of cement suspensions: rheometry, Computational Fluid Dynamics Modeling and field test measurements", *Cement and Concrete Research*, 42, pp. 1134-1146.

[93] Ferrara, L. and Haist, M. (2012), "Rheological characterization of High Performance Fiber Reinforced Cementitious Composites", in J. Barros et al. eds., Proceedings BEFIB 2012, Guimaraes, Portugal, September 20-22, 2012, RILEM Pubs., 12 pp.

[94] Baril, M.A., Sorelli, L., Réthoré, J., Baby, F., Toutlemonde, F., Ferrara, L., Bernardi, S. and Fafard, M. (2016), "The Effect of Casting Flow Defects on the Crack Propagation of UHPFRC Thin Slabs by Stereovision Digital Image Correlation", Construction and Building Materials (2016), *in press*, http://dx.doi.org/10.1016/j.conbuildmat.2016.10.102

Figures

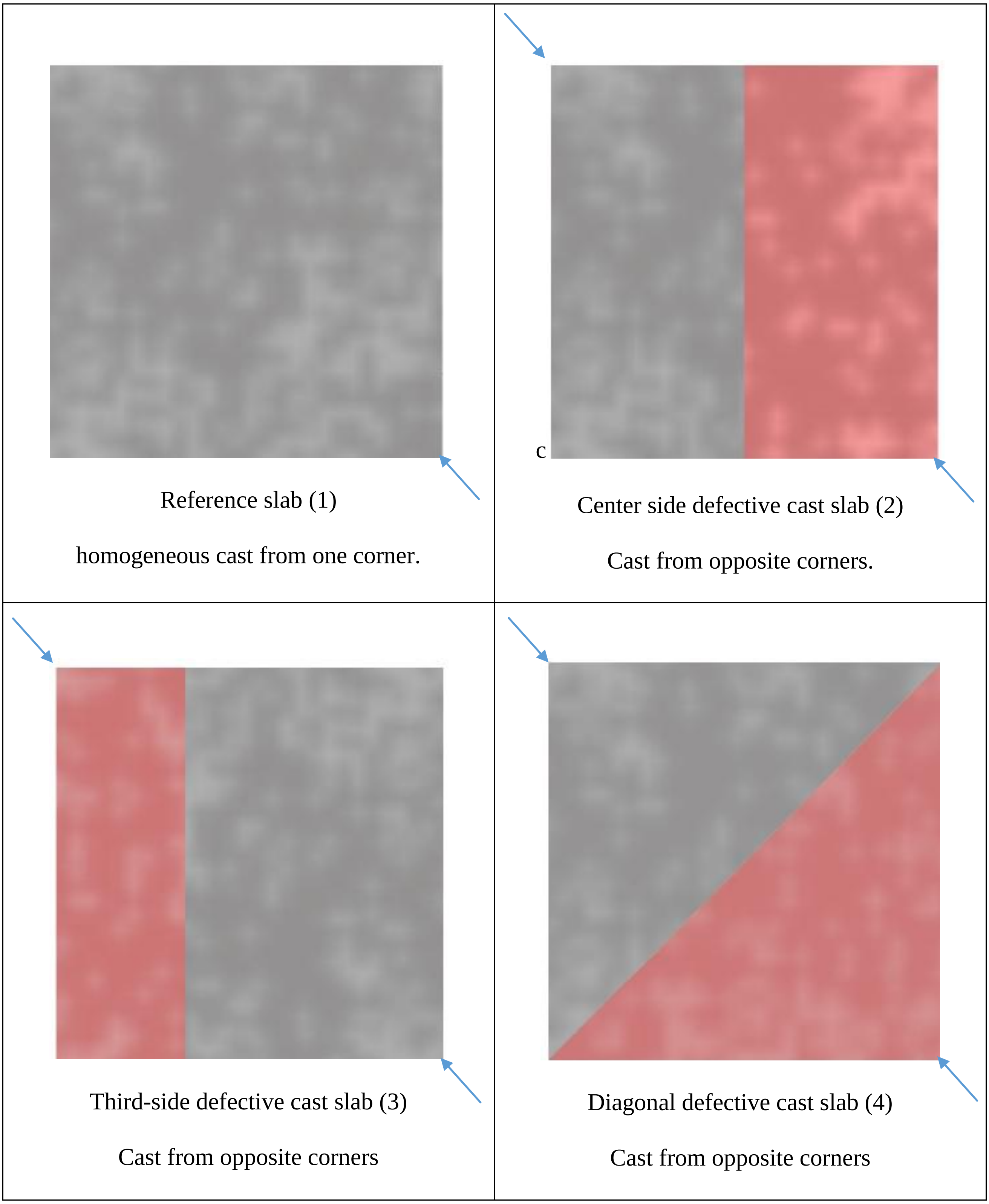

Figure 1: schematic of investigated slabs with position of pre-arranged defect – arrows indicate the pouring points and directions of the fresh HPFRCC mixture.

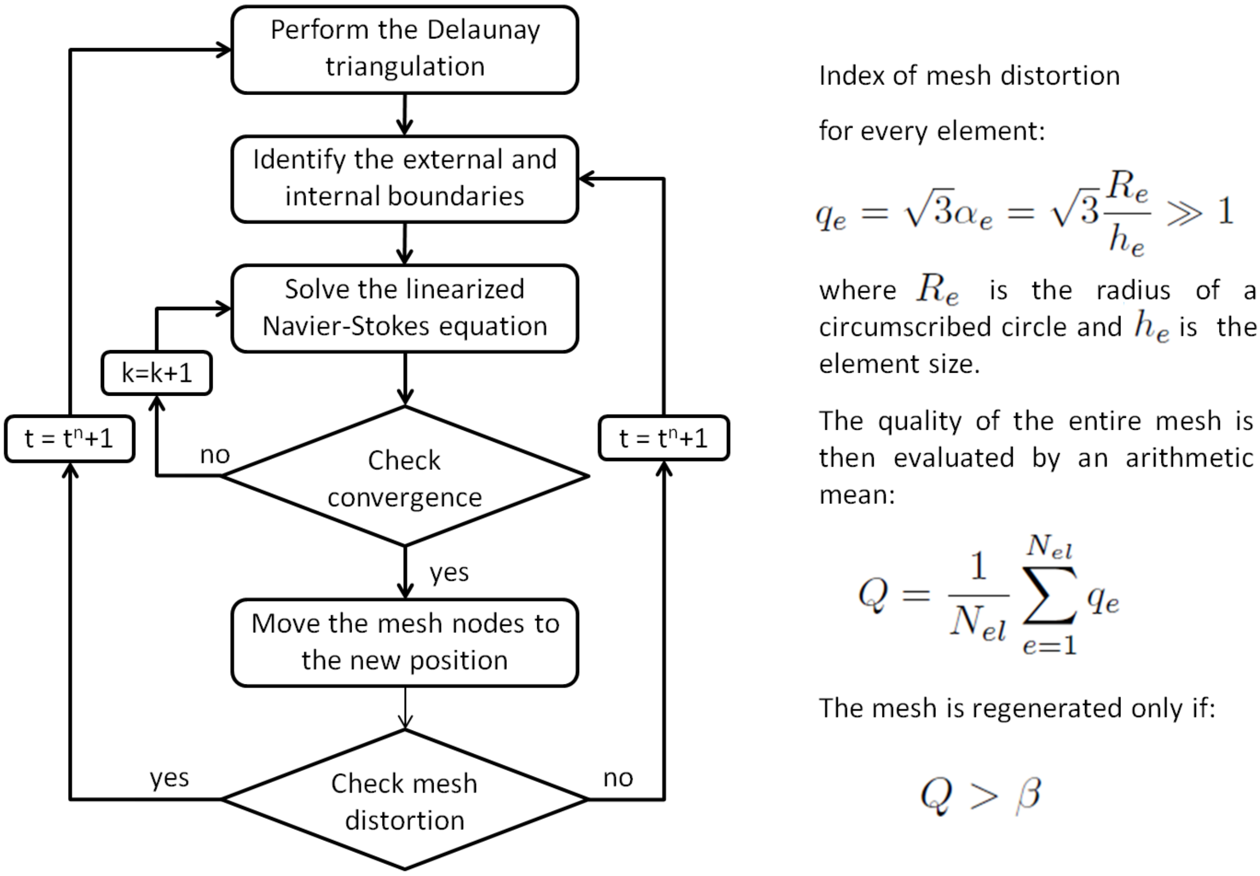

Figure 2: flow chart of the employed numerical approach including re-meshing scheme based on mesh distortion.

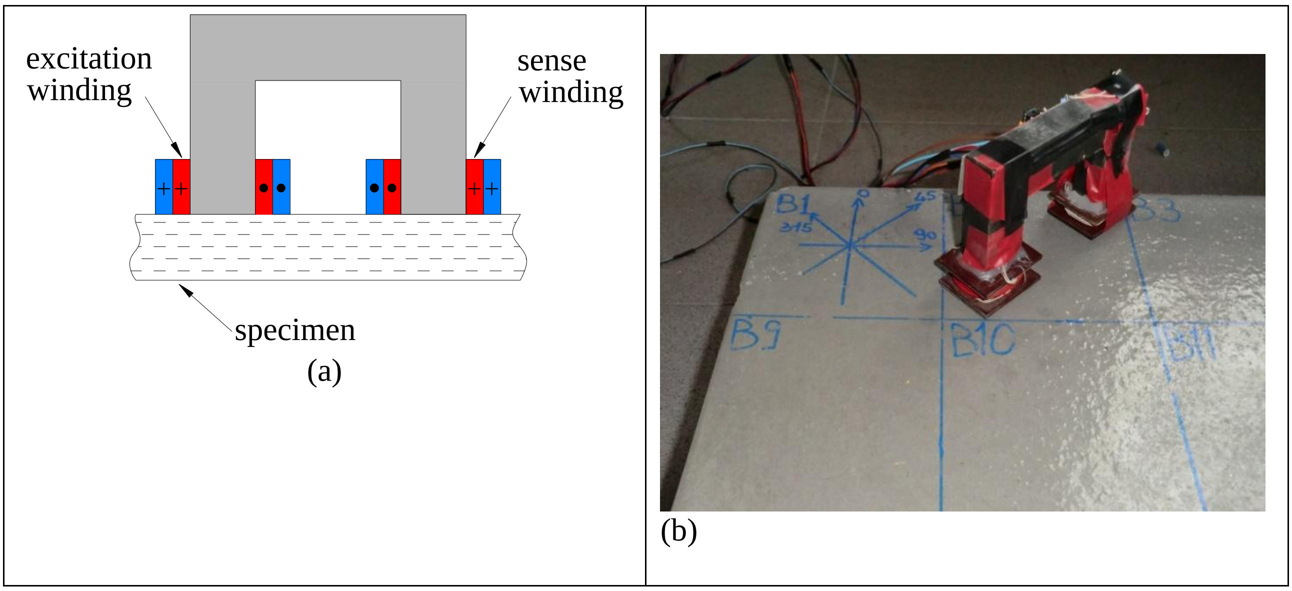

Figure 3. Schematic (a) and picture (b) of the two winding probe employed for non-destructive magnetic survey of fiber dispersion.

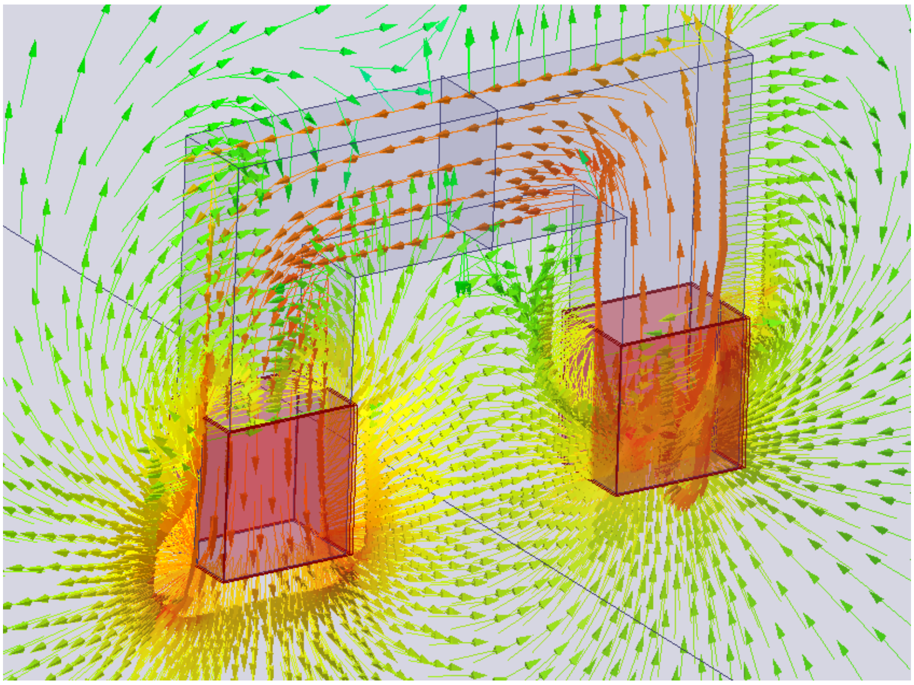

Figure 4. Two winding probe: flux density predicted by FEM analysis.

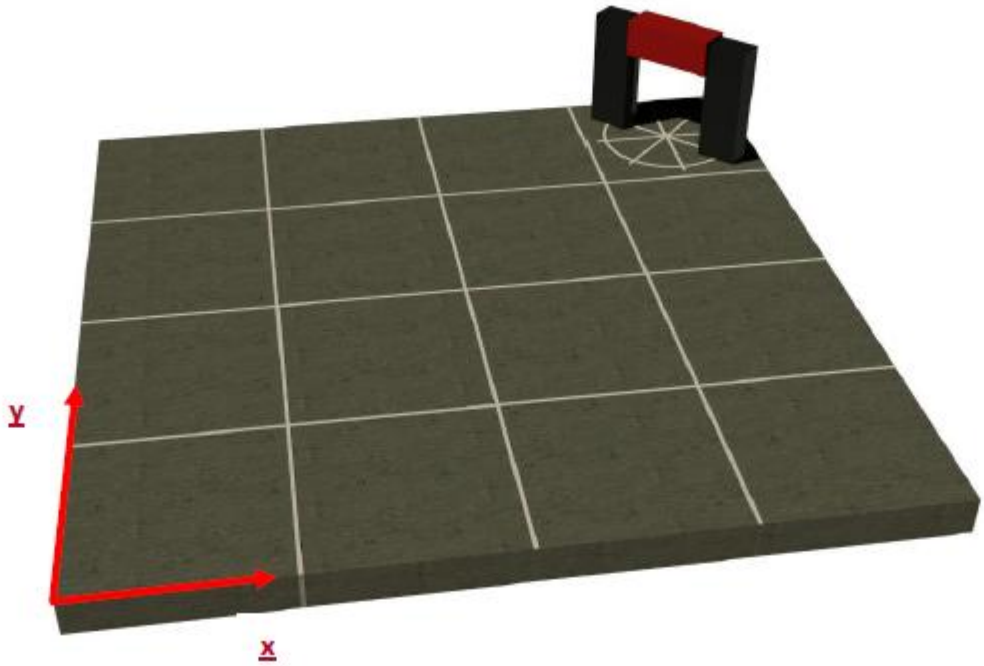

(a)

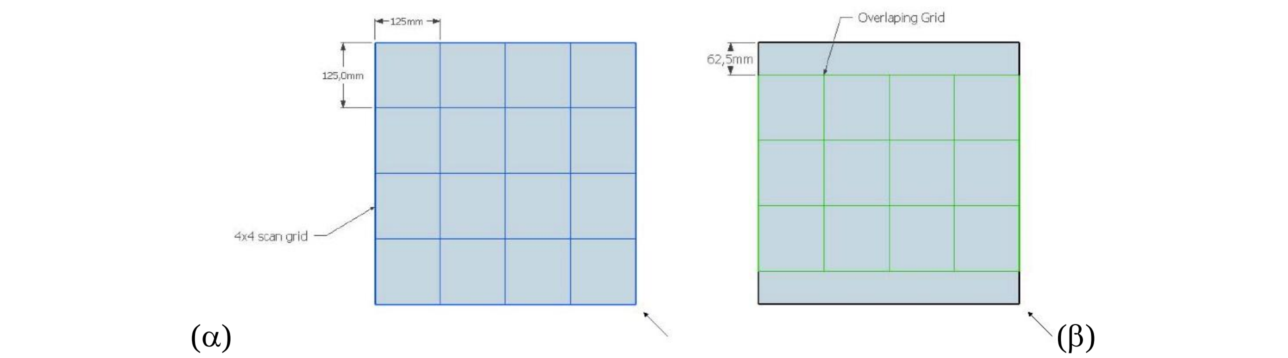

(b) - Reference slab (1) - homogeneous cast from one corner: overall (α) and partial grid (β).

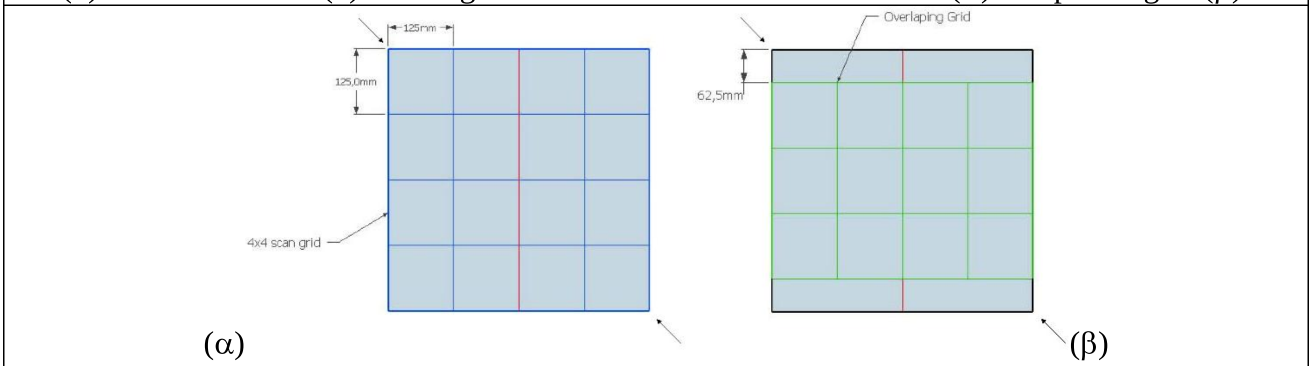

(c) - Center side defective slab (2) - cast from opposite corners: overall (α) and partial (β) grid.

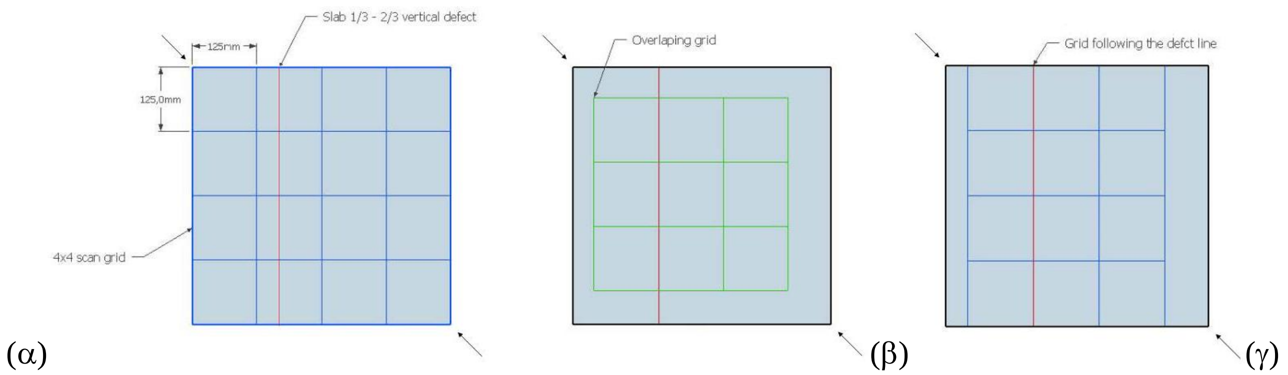

(d) - Third-side defective slab (3) - Cast from opposite corners: overall (α) and partial (β,γ) grids.

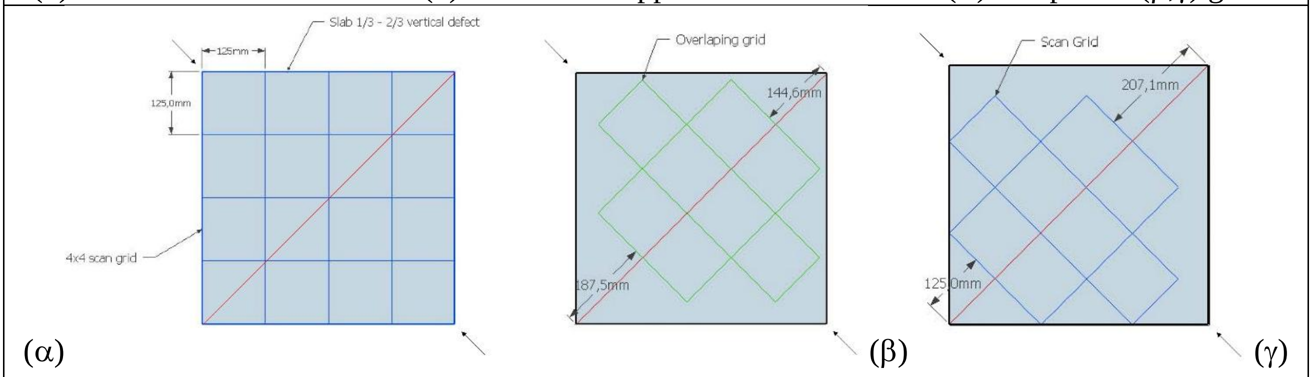

(e) - Diagonal defective slab (4) - Cast from opposite corners: overall (a) and partial (β,γ) grids.

Figure 5: schematic of the non-destructive measuring set-up, with x-y reference axes highlighted,(a) and details of the cell schematics employed for each of the investigated HPFRCC slabs (b-e) – arrows indicate the pouring points and directions of the fresh HPFRCC mixture and solid lines indicate position of prearranged defects.

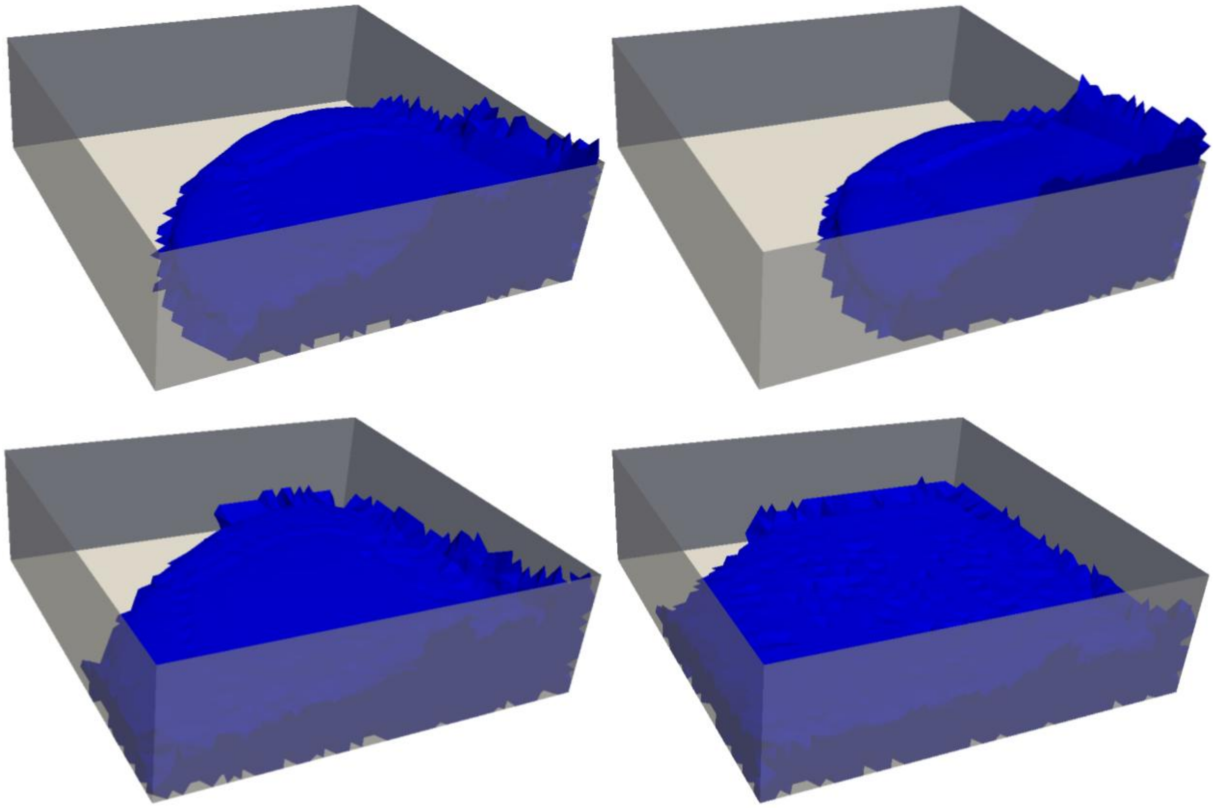

(a) – reference slab with no casting defect

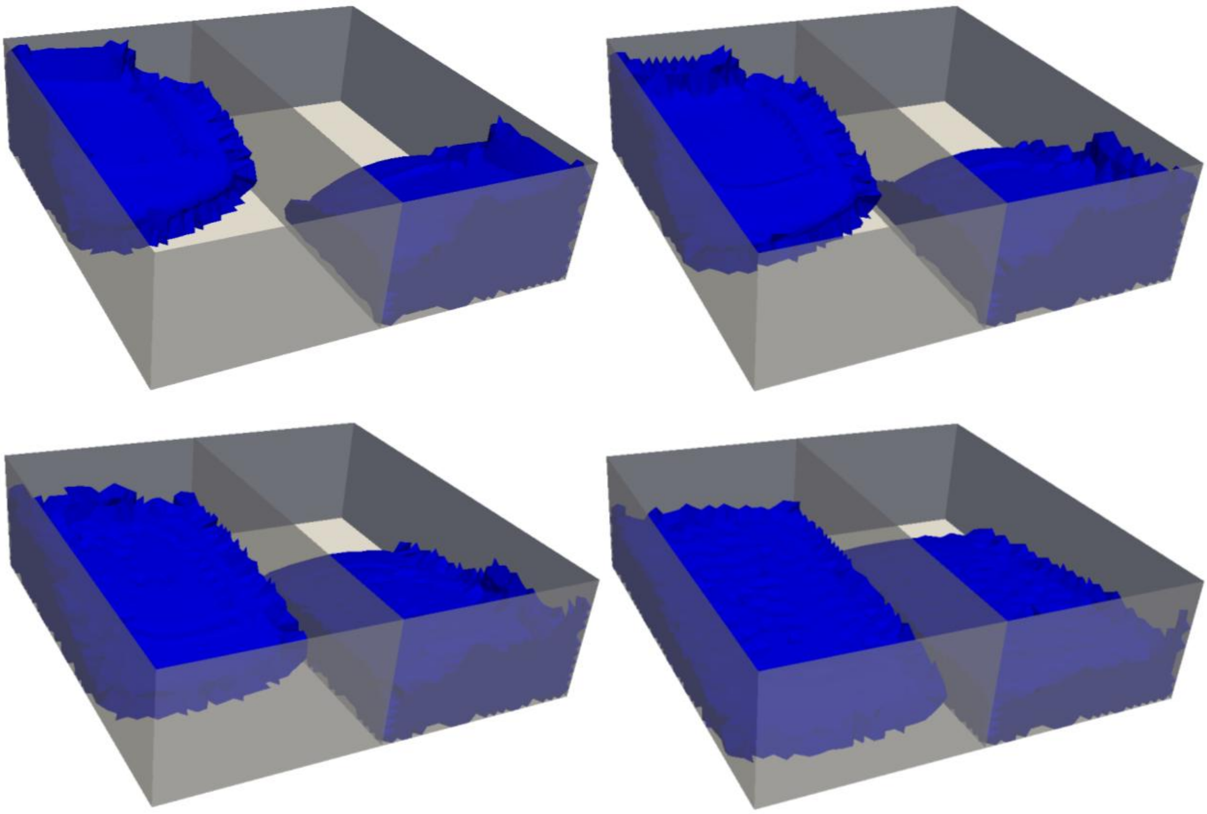

(b) – center side defective slab

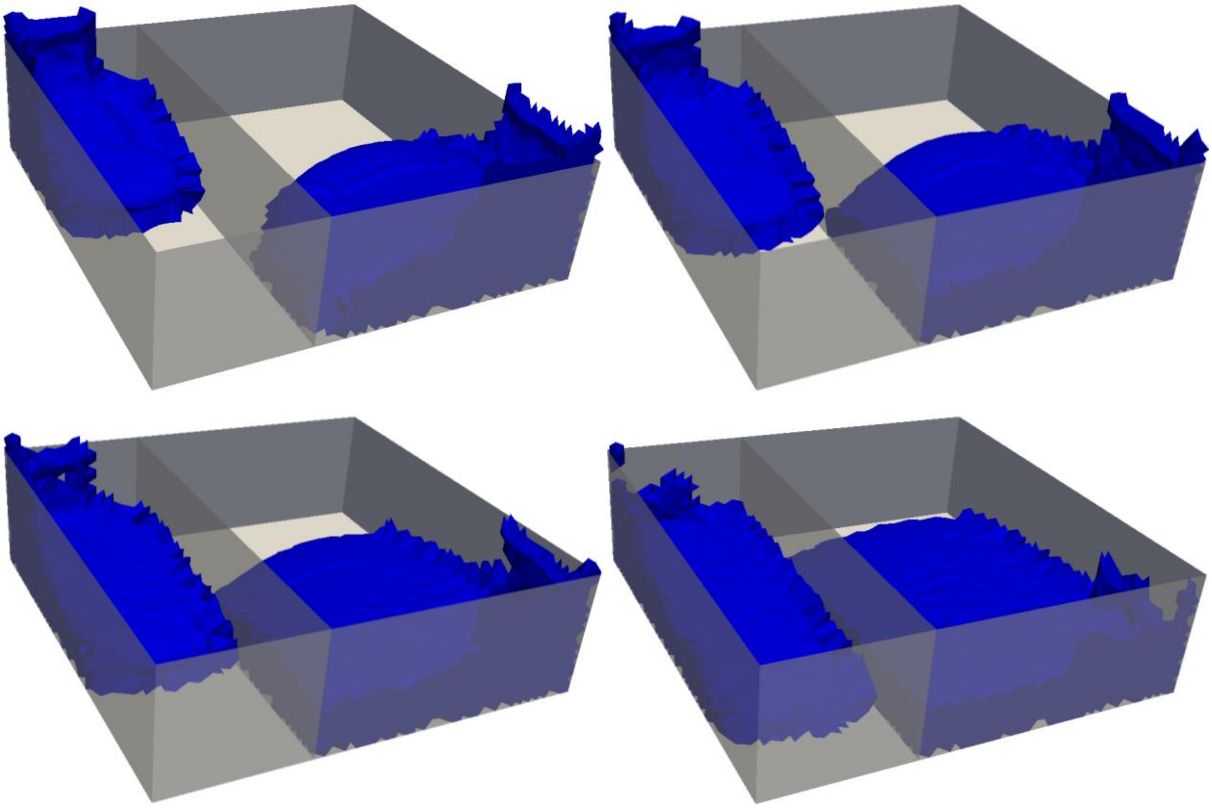

(c)- third side defective slab

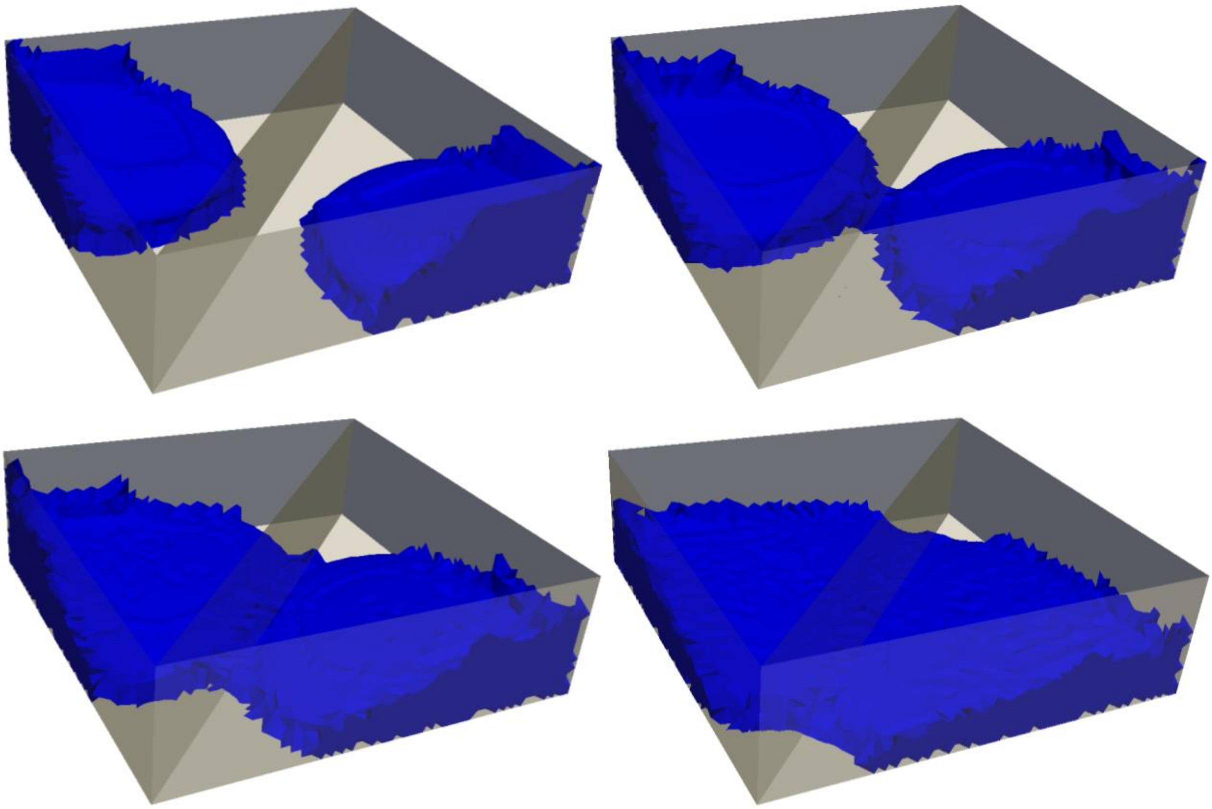

(d)– diagonal defective slab

Figure 6: snapshots of simulated casting processes

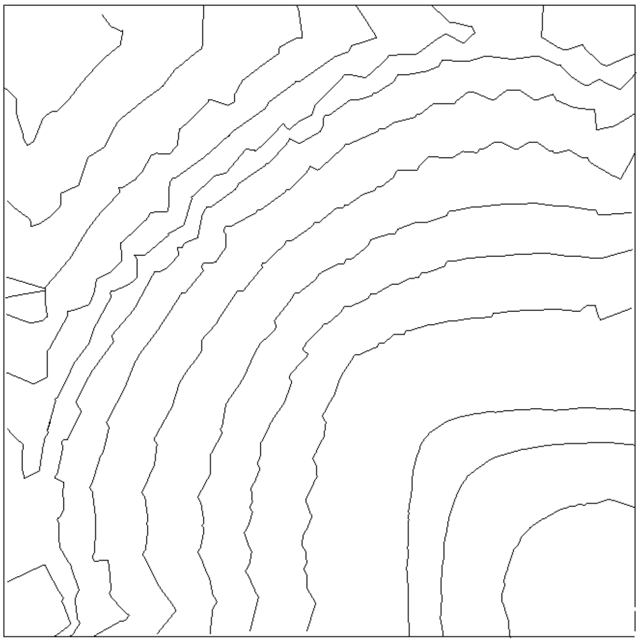

(a)- Reference slab (1)

homogeneous cast from one corner.

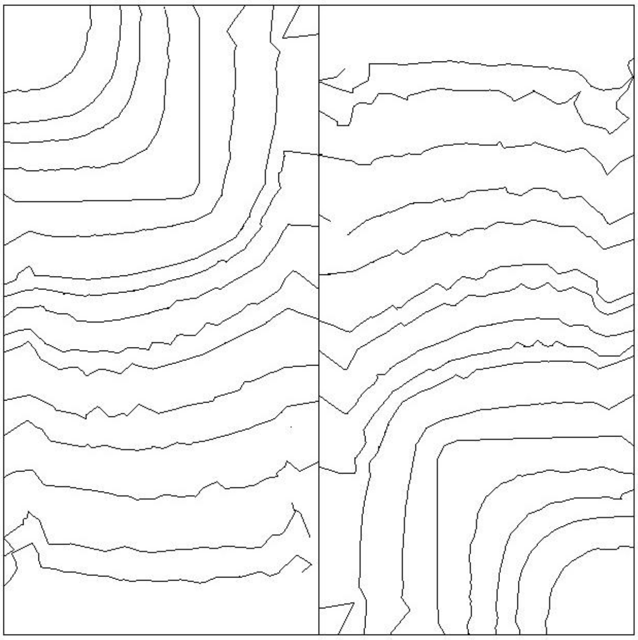

(b) - Center side defective cast slab (2)

Cast from opposite corners.

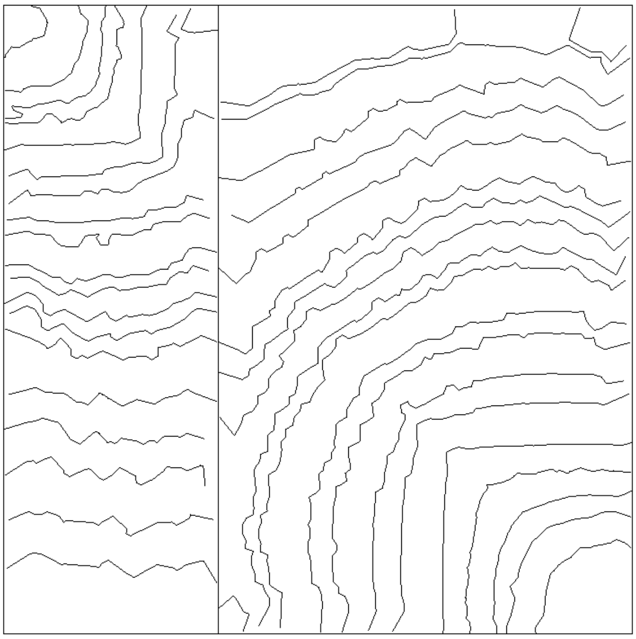

(c) - Third-side defective cast slab (3)

Cast from opposite corners

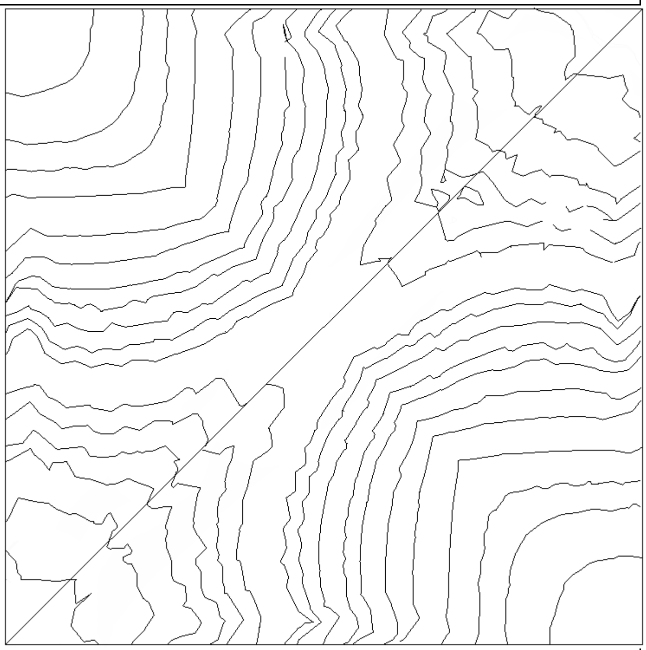

(d)- Diagonal defective cast slab (4)

Cast from opposite corners

Figure 7: envelope lines of the advanced fluid front in simulated casting flow process of the investigated HPFRCC slabs

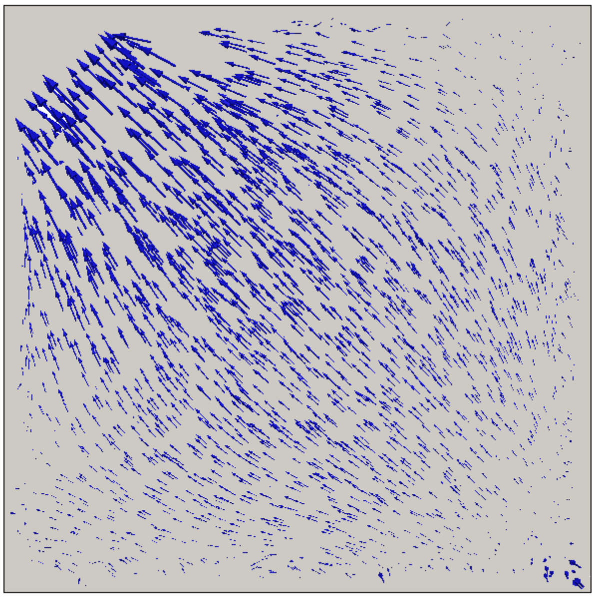

(e) - Reference slab (1)

homogeneous cast from one corner.

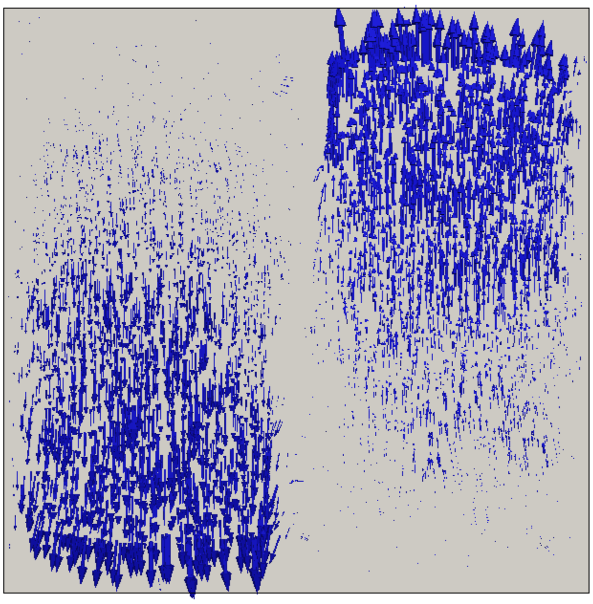

(f) - Center side defective cast slab (2)

Cast from opposite corners.

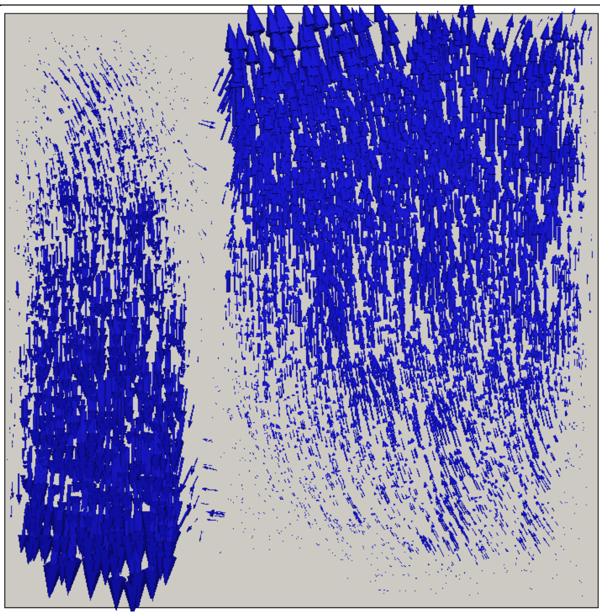

(g)- Third-side defective cast slab (3)

Cast from opposite corners

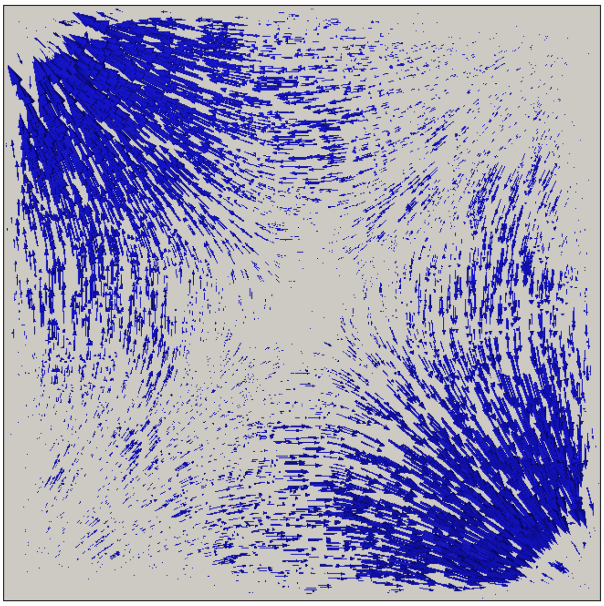

(h) - Diagonal defective cast slab (4)

Cast from opposite corners

Figure 7 ctd.: velocity field vectors in simulated casting processes of the investigated HPFRCC slabs.

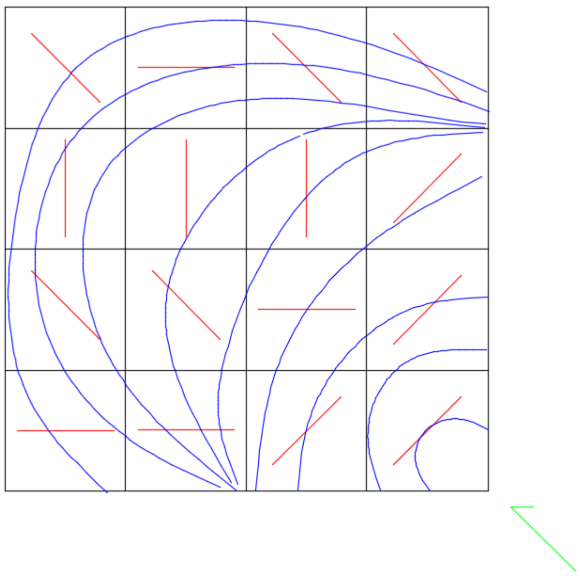

Reference slab (1)

homogeneous cast from one corner.

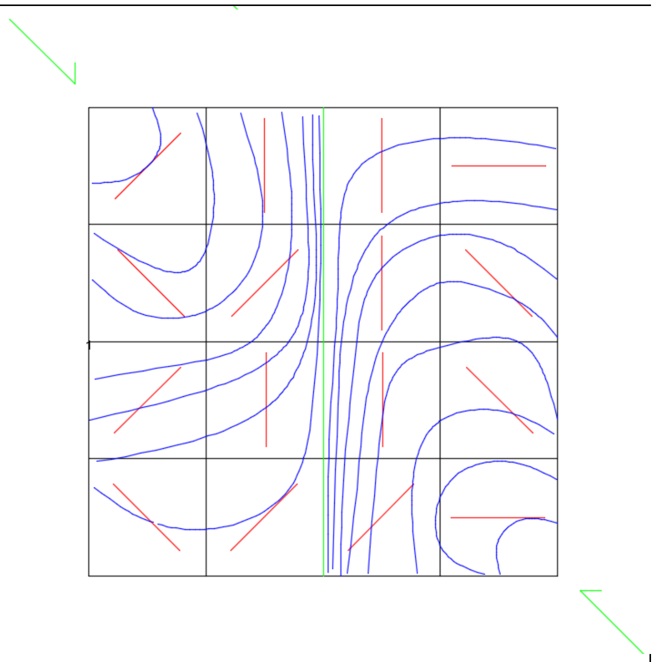

Center side defective cast slab (2)

Cast from opposite corners.

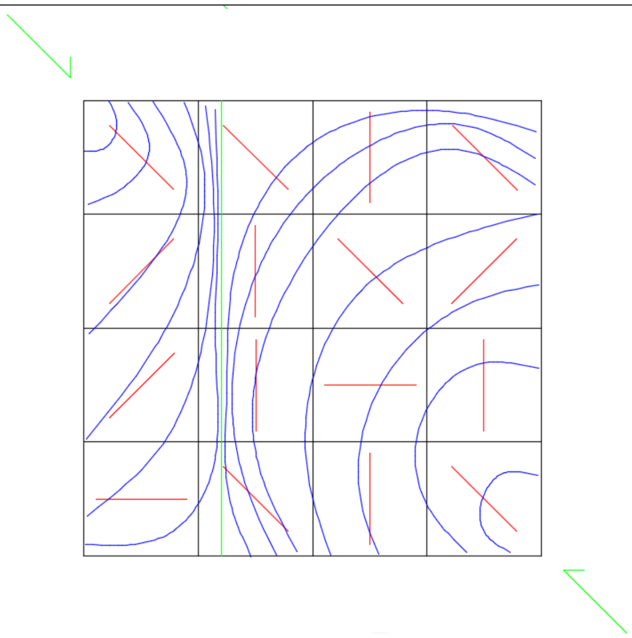

Third-side defective cast slab (3)

Cast from opposite corners

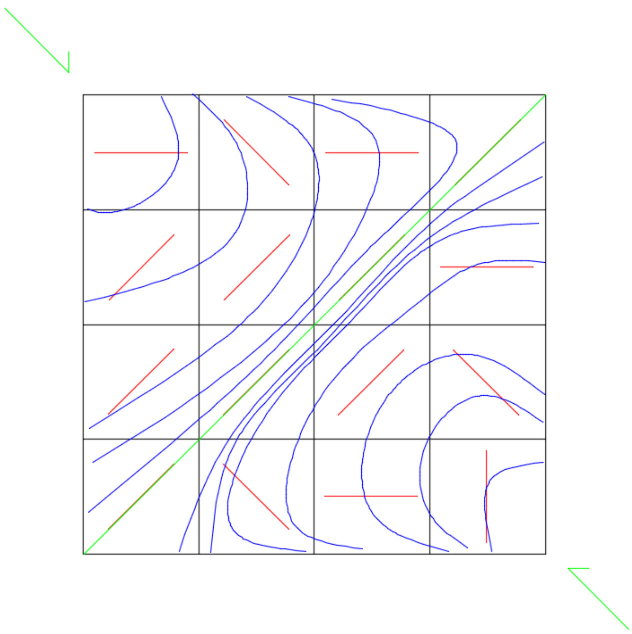

Diagonal defective cast slab (4)

Cast from opposite corners

Figure 8: matching between directions of maximum measured compensated inductance (red segments) and simulated advance of casting flow front for the four investigated HPFRCC slabs.

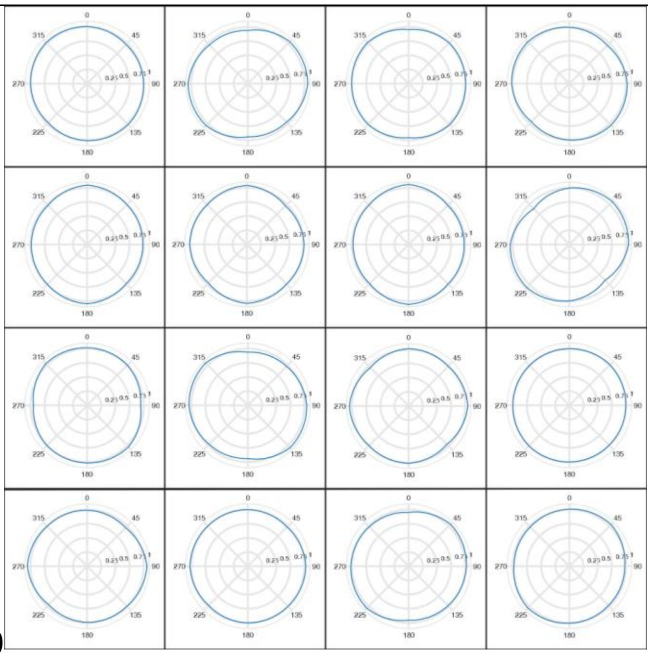

(α)

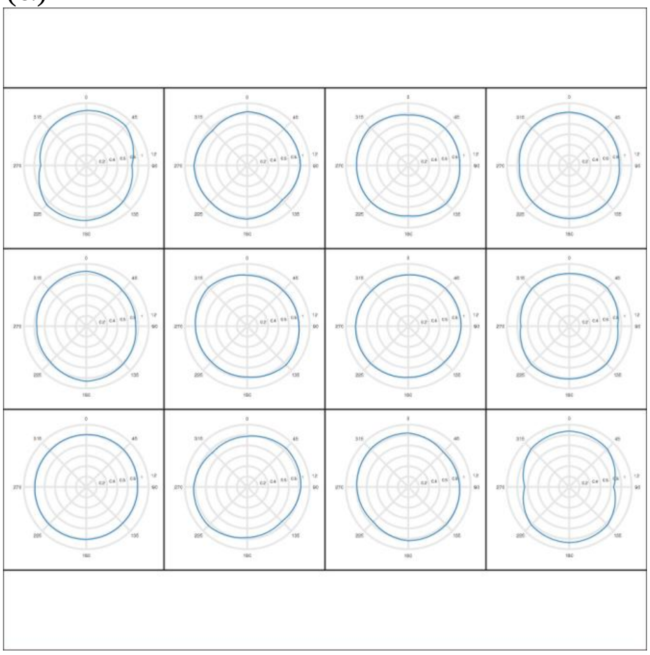

(β)

(a) - Reference slab (1) - homogeneous cast from one corner: overall (α) and partial grid (β).

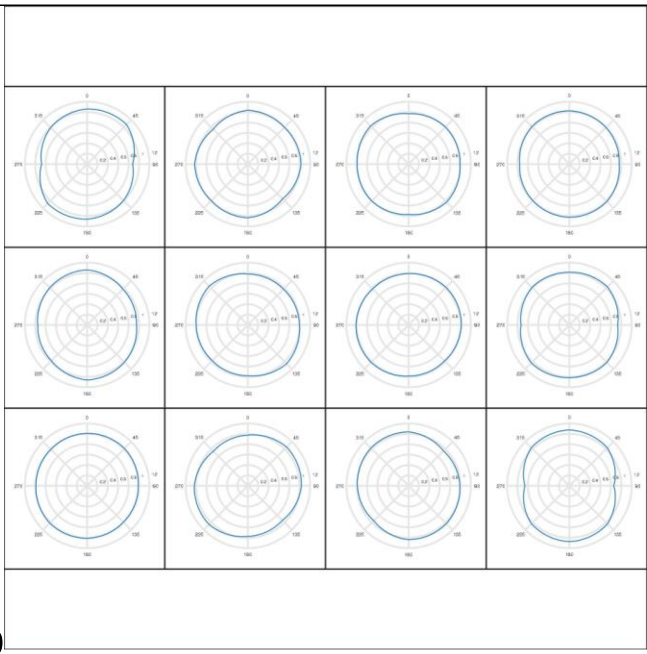
(α)

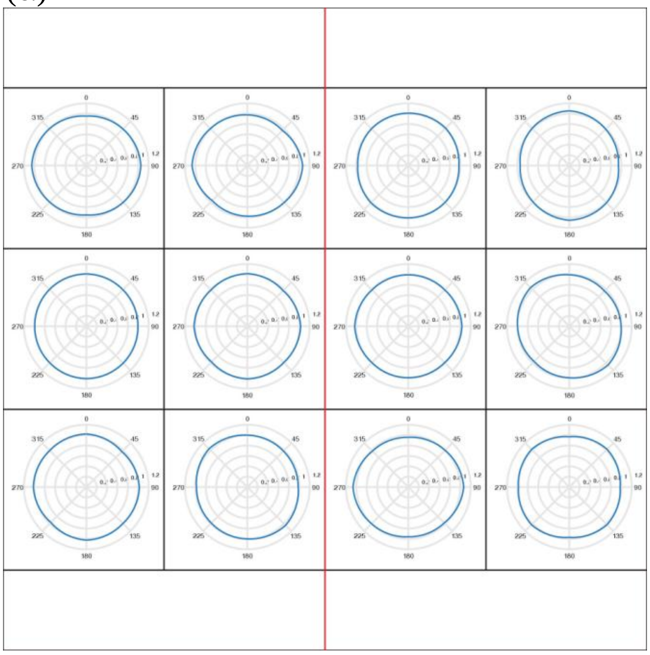

(β)

(b) - Center side defective slab (2) - cast from opposite corners: overall (α) and partial (β) grid.

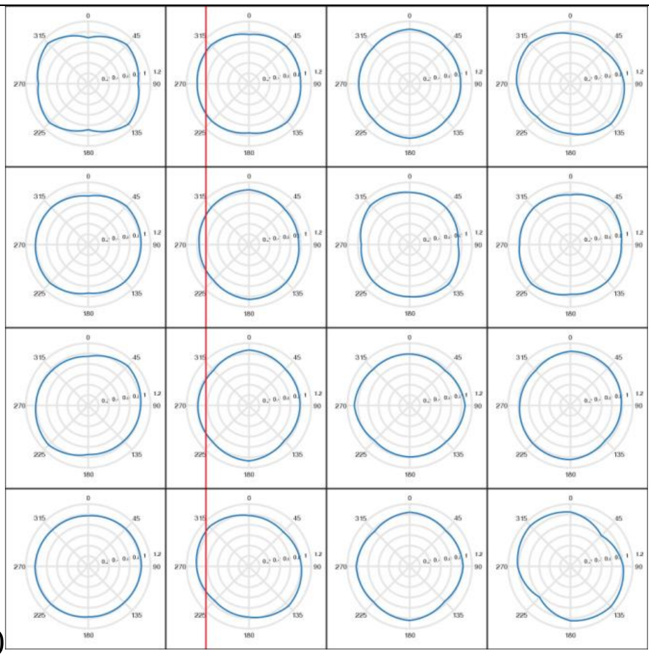

(α)

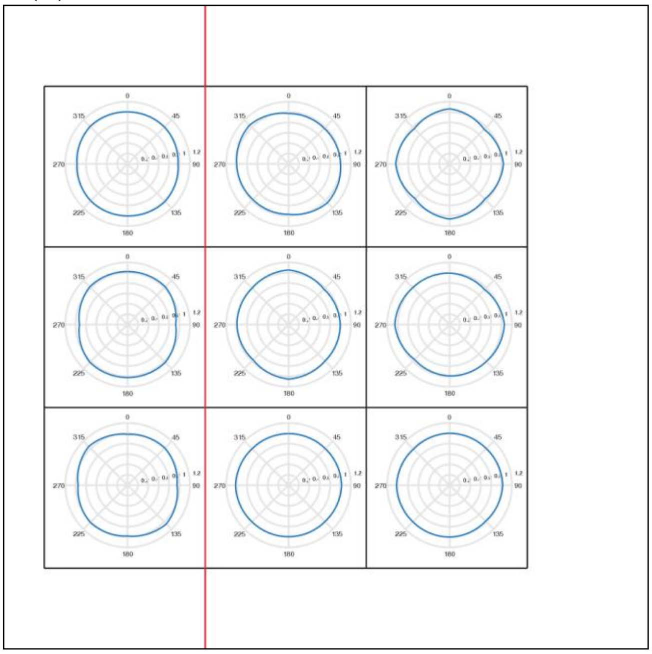

(β)…..

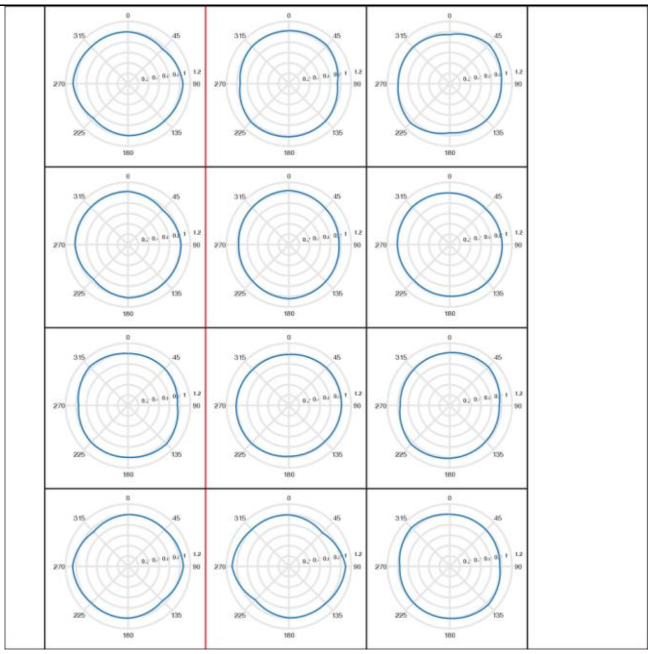

(γ)

(c) - Third-side defective slab (3) - Cast from opposite corners: overall (α) and partial (β,γ) grids.

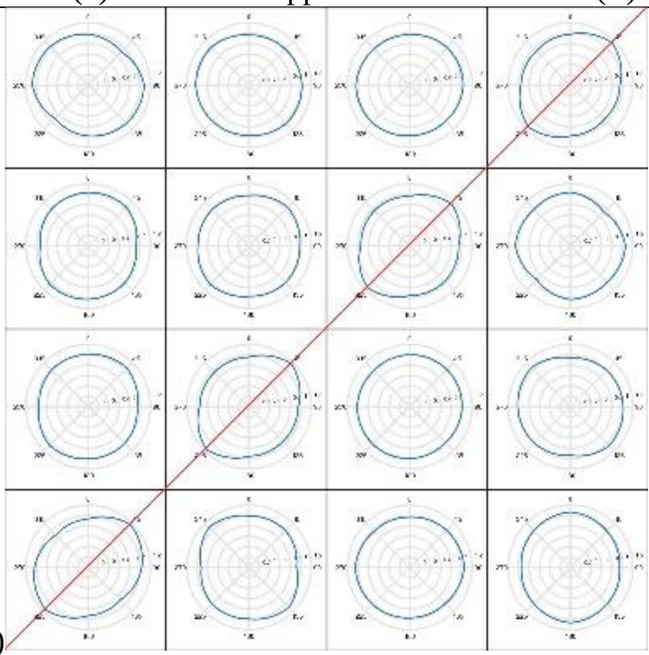

(α)

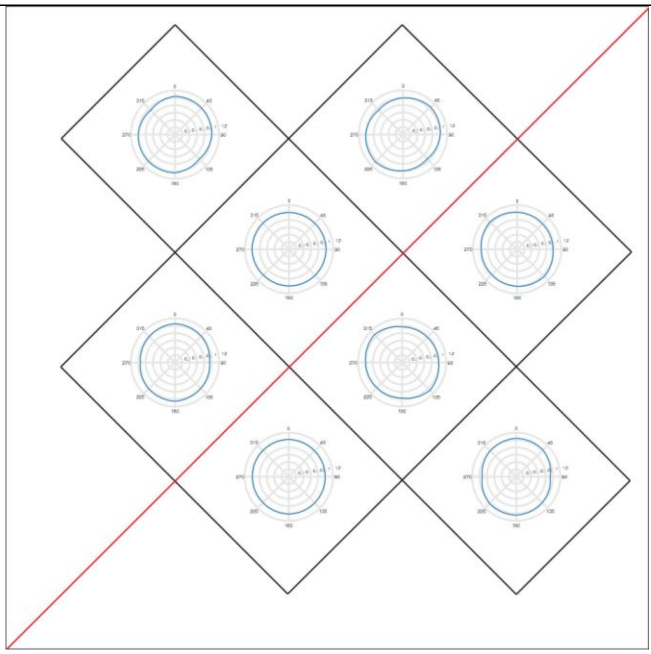

(β)

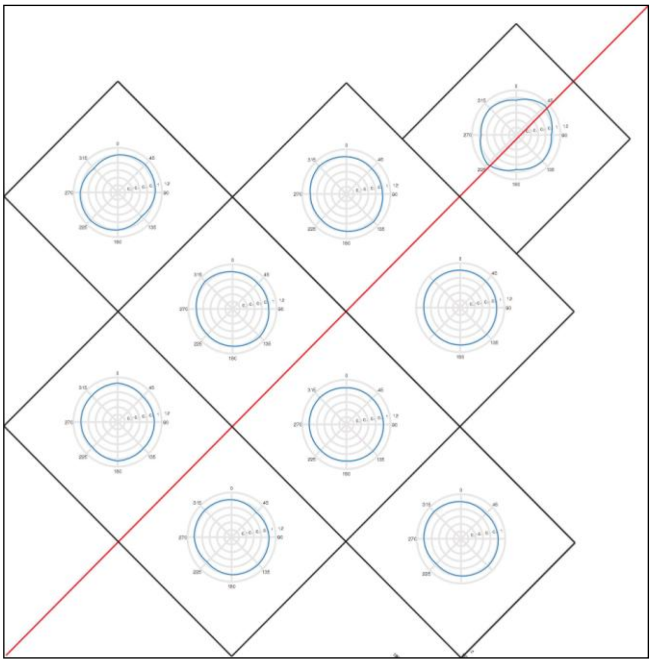

(γ)

(d) - Diagonal defective slab (4) - Cast from opposite corners: overall (a) and partial (β,γ) grids.

Figure 9: polar plots of local anisotropies in fiber orientation as from non-destructive magnetic survey for the four investigated HPFRCC slabs.

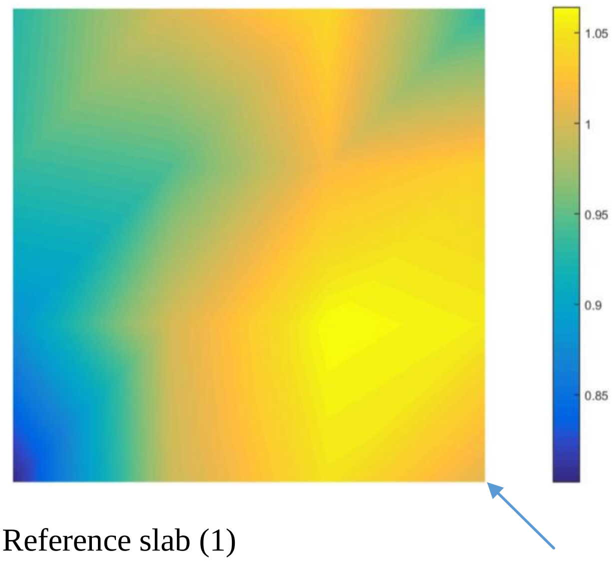

Reference slab (1)

homogeneous cast from one corner.

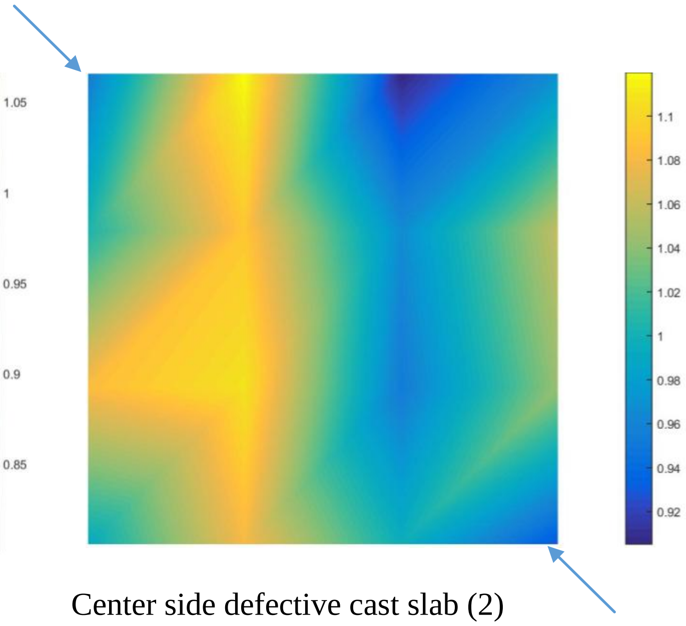

Center side defective cast slab (2)

Cast from opposite corners.

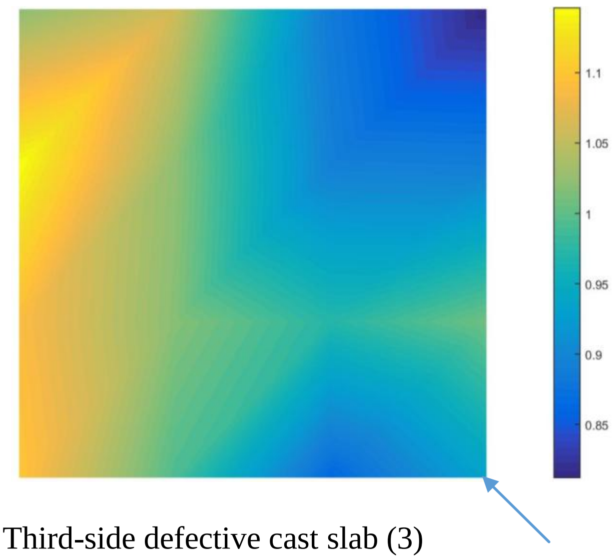

Third-side defective cast slab (3)

Cast from opposite corners

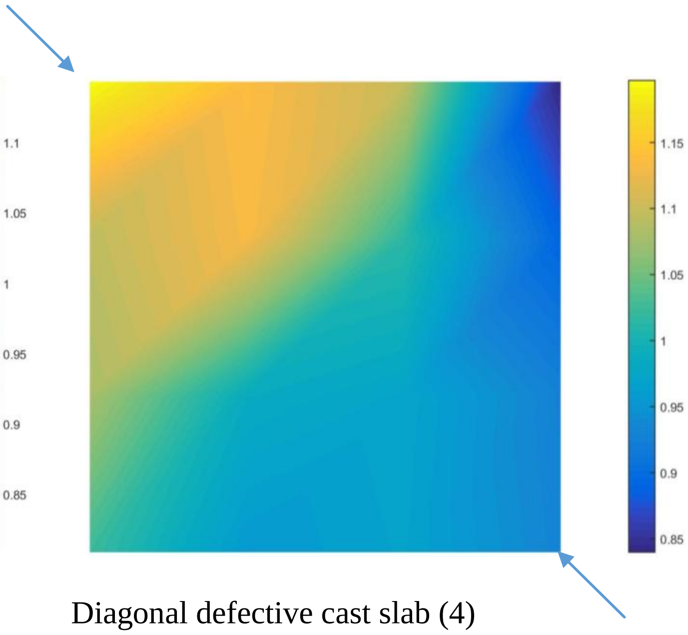

Diagonal defective cast slab (4)

Cast from opposite corners

Figure 10: estimation of homogeneity in fiber distribution content in the four investigated HPFRCC slabs – values of the homogeneity parameter higher/lower than 1 will indicate fiber content higher/lower than nominal reference one – arrows indicate pouring points and directions.

*

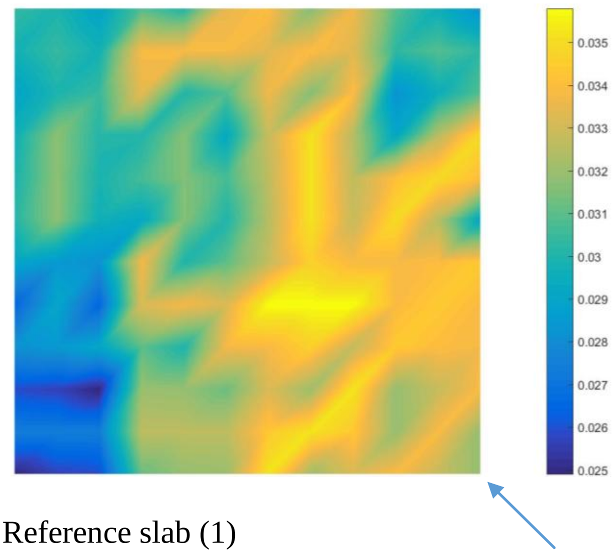

Reference slab (1)

homogeneous cast from one corner.

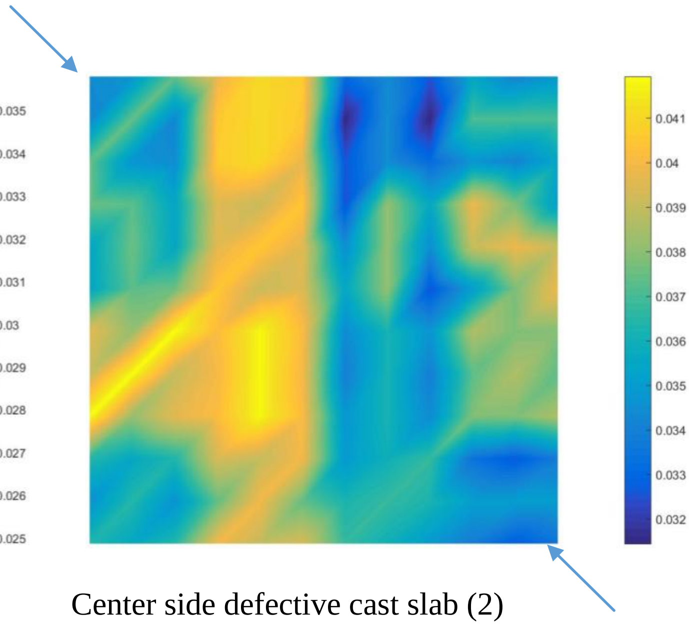

Center side defective cast slab (2)

Cast from opposite corners.

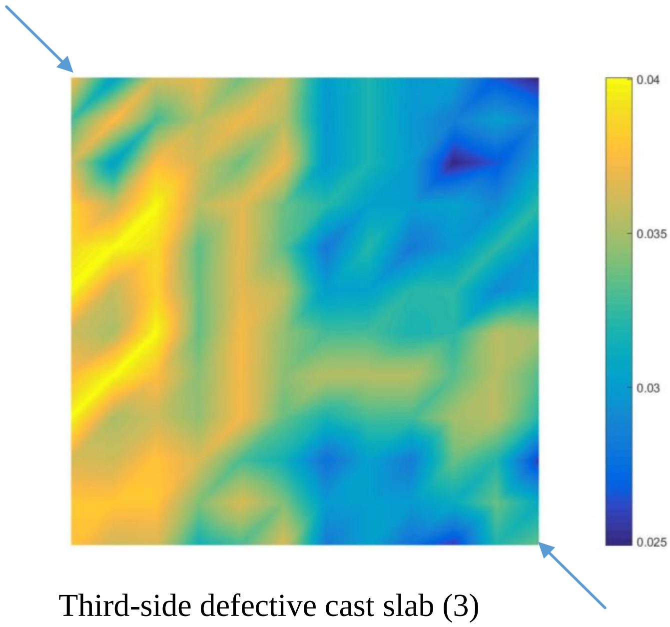

Third-side defective cast slab (3)

Cast from opposite corners

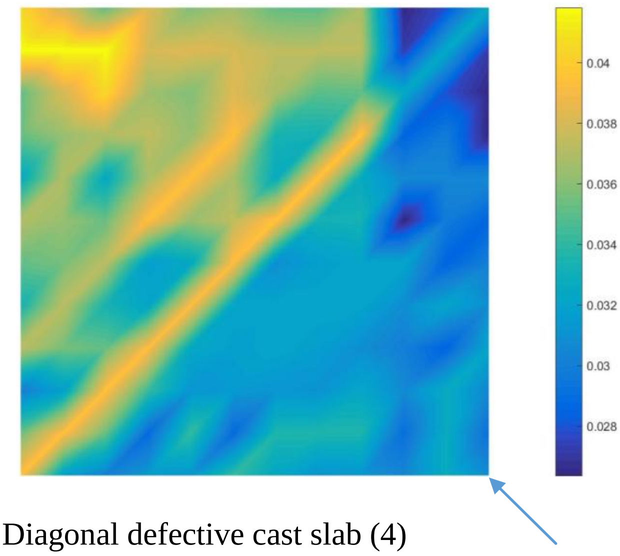

Diagonal defective cast slab (4)

Cast from opposite corners

Figure 11: estimation of homogeneity in fiber distribution content and orientation in the four investigated HPFRCC slabs – higher values of the compensated inductance indicate higher concentration of fibers along the plotted direction – arrows indicate pouring points and directions.

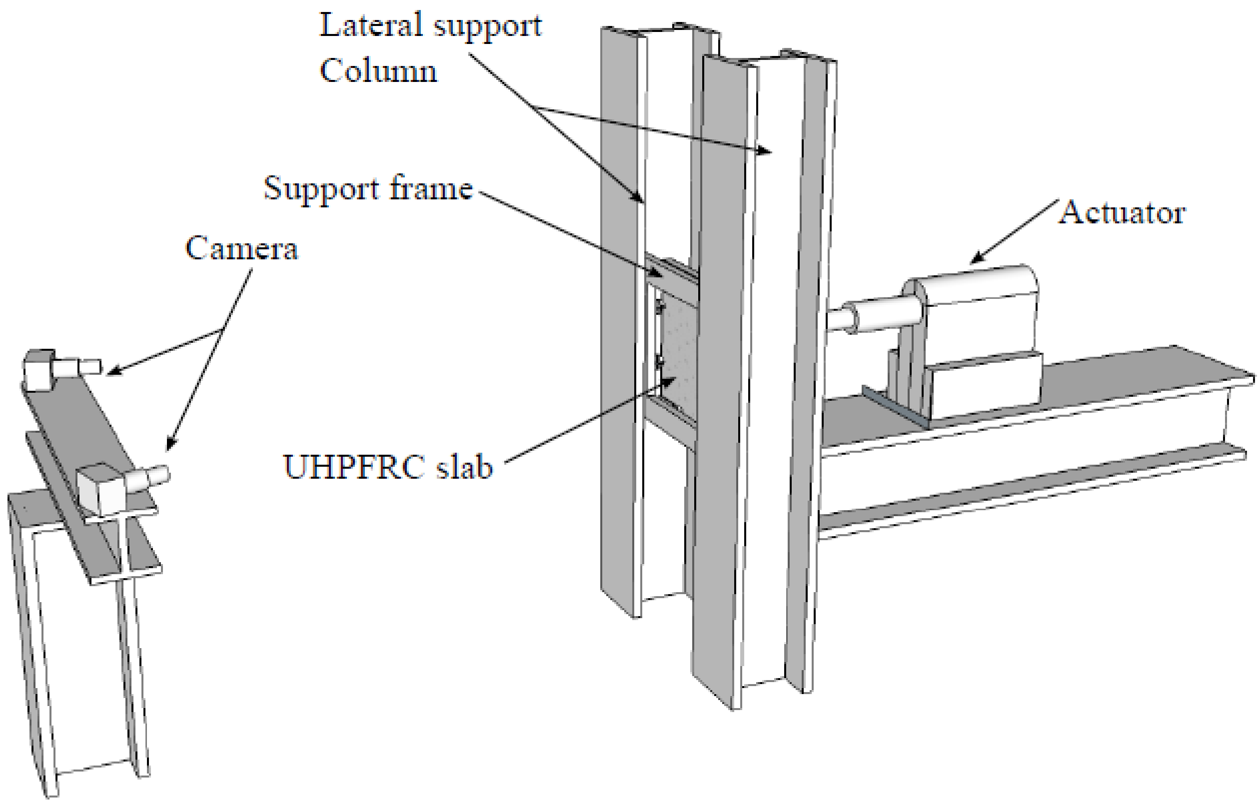

Figure 12: schematic of the test set-up and stereo-vision digital image correlation system employed for mechanical tests on surveyed UHPC slabs.

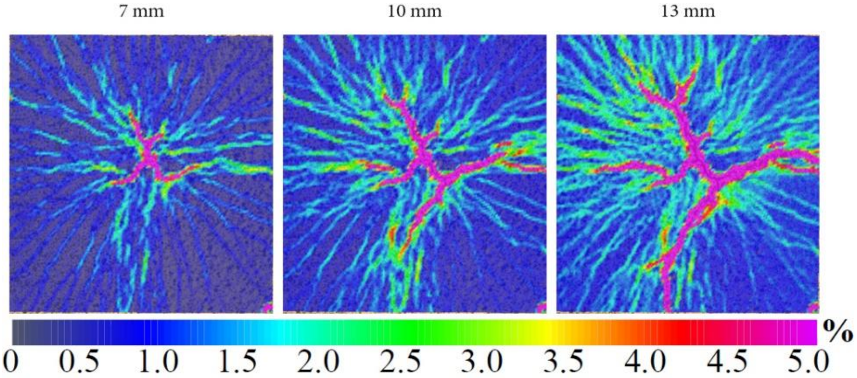

(a) - Reference slab (1) - homogeneous cast from one corner.

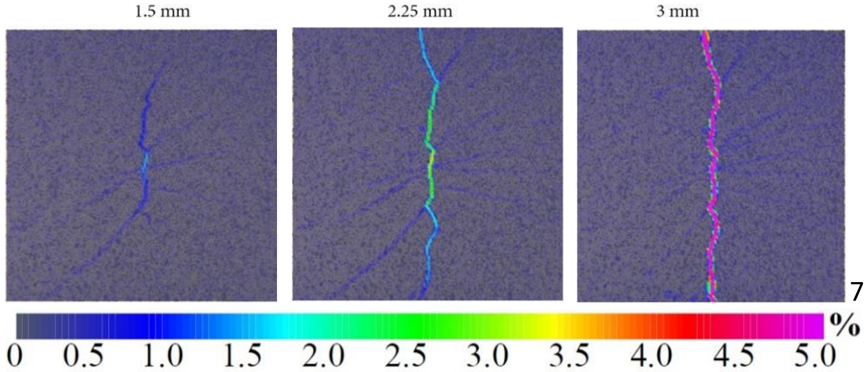

(b) - Center side defective slab (2) - cast from opposite corners.

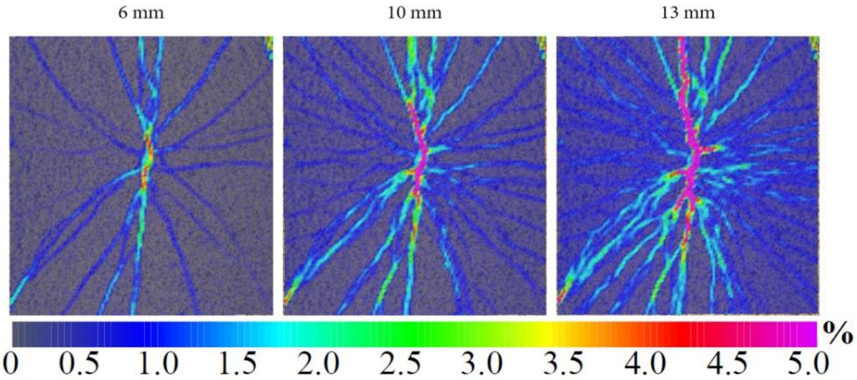

(c) - Third-side defective slab (3) - cast from opposite corners.

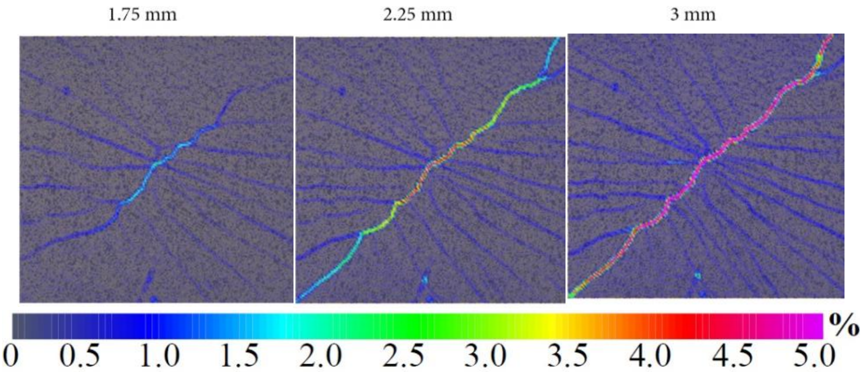

(d) - Diagonal defective slab (4) - Cast from opposite corners.

Figure 13: evolution of crack and deformation patterns during load tests for the four investigated HPFRCC slabs.

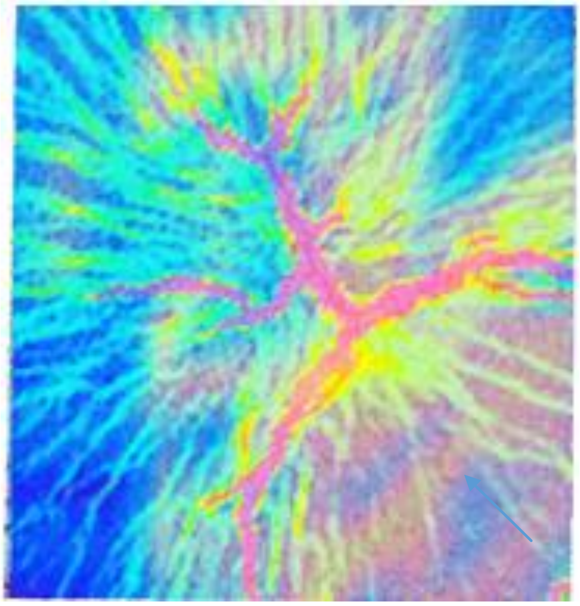

Reference slab (1)

homogeneous cast from one corner.

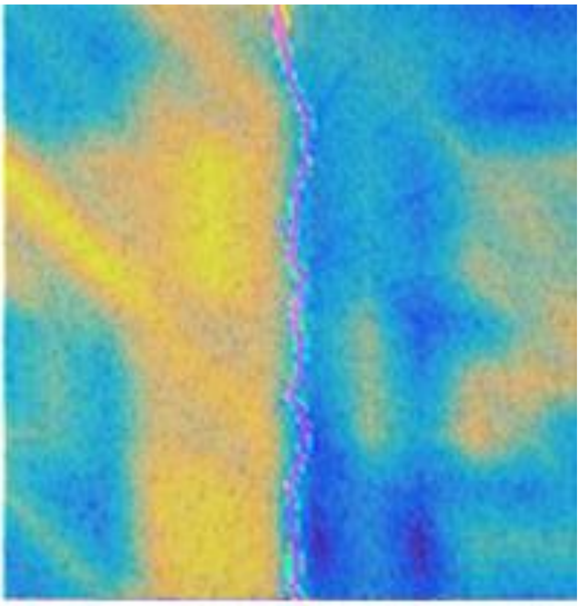

Center side defective cast slab (2)

Cast from opposite corners.

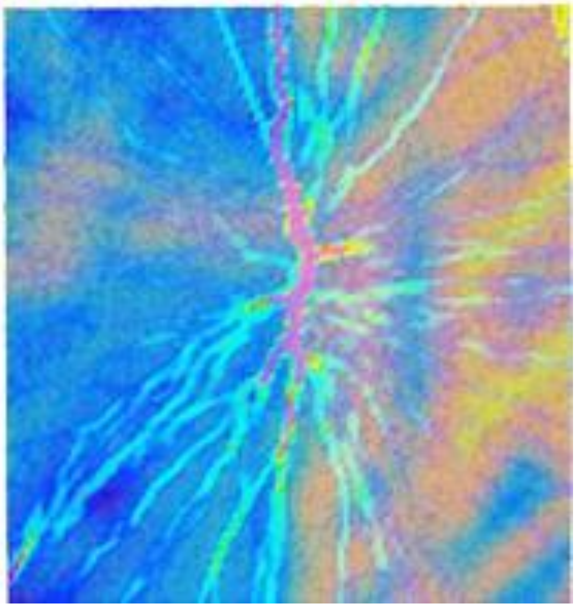

Third-side defective cast slab (3)

Cast from opposite corners

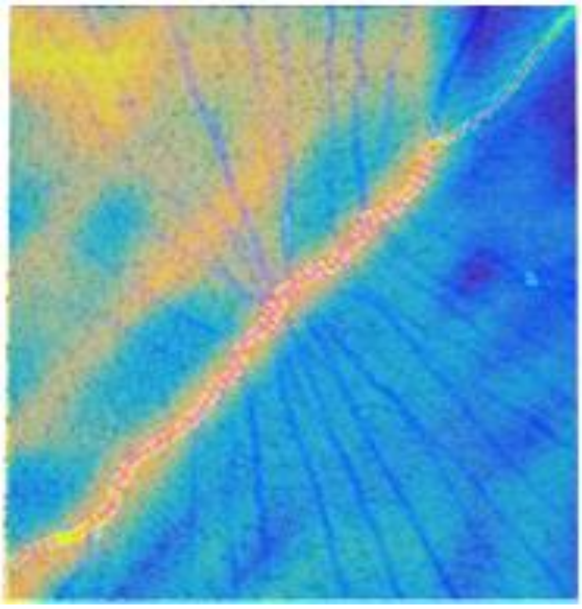

Diagonal defective cast slab (4)

Cast from opposite corners

Figure 14: superposition between fiber dispersion and homogeneity plots and crack patterns at failure for the four investigated HPFRCC slabs.